errors in the true coincidences. The statistical errors from photopeak-separation uncertainties were included. We noted that the 2.12-MeV branch, for which the photopeak is practically free from 1.81-MeV γ's, gave unity for the value of χ^2 (about the mean ϵ), divided by the number of runs.

The average values of ϵ for the 1.81- and 2.12-MeV mixed γ transitions are $(-4.3\pm2.5)\times10^{-4}$ and $(-3.8\pm2.0)\times10^{-4}$, respectively. In Table I, these results are translated into values of $|\delta|\sin\eta$, $\sin\eta$, and η. We feel that our nonzero values of ϵ arise from asymmetries in experimental conditions, and that the difference in asymmetries give a more bias-free measure of a possible T-violation effect. A nonzero difference would imply that nonvanishing asymmetry terms are actually present and that T invariance is violated. We find a difference, $\Delta\epsilon=(0.4\pm3.2)\times10^{-4}$, and conclude *that no evidence for time-reversal violation is present.*

The standard deviation in the experimental value of the asymmetry difference can be translated into an error in the determination of the phase η. The difference in imaginary parts of the mixing ratio is about 19 times ϵ; $\Delta(|\delta|\sin\eta)\cong(1\pm6)\times10^{-3}$. Although the difference $\Delta\sin\eta$ in imaginary parts of the complex phase is not proportional to $\Delta(|\delta|\sin\eta)$ because $|\delta|$ is not the same for both cascades, we can use the average mixing ratio $\langle|\delta|\rangle=0.23$ in order to estimate it and find $\Delta\eta\cong\Delta\sin\eta\cong(0.4\pm2.6)\times10^{-2}$.

ACKNOWLEDGMENTS

It is a pleasure to thank G. Beck, P. Hesselman, and S. Boudreaux for their untiring help in the preparation of the ^{56}Mn sources. We also thank the Physics Research Laboratory Staff for the use of facilities and apparatus, and Dr. A. Wattenberg for the loan of modular electronics.

PHYSICAL REVIEW VOLUME 187, NUMBER 4 20 NOVEMBER 1969

Properties of P^{30} Levels from the Reaction $Si^{29}(p, \gamma)P^{30}$. II

GALE I. HARRIS, A. K. HYDER, JR., AND J. WALINGA*
Aerospace Research Laboratories,† Wright-Patterson Air Force Base, Ohio 45433
(Received 5 December 1968)

A previous investigation of the γ-ray decay schemes of 7 resonances in the reaction $Si^{29}(p, \gamma)P^{30}$ in the range $E_p=700$–1750 keV has been extended to 24 resonances in the range $E_p=300$–1800 keV. The new decay scheme studies were conducted with a 40-cc Ge(Li) detector. The spins, parities, isobaric spins, lifetimes, and transition multipolarity mixings for many resonances and bound states of P^{30} have been determined from an extensive series of angular-correlation, linear-polarization, and Doppler-shift-attenuation measurements. New resonance information includes the discovery that resonances previously reported at $E_p=1505$, 1748, and 1772 keV are each doublets. The latter two have components at 1746 and 1749, and at 1773 and 1775 keV, respectively. The 1505-keV "resonance" was found to be a doublet with a separation of 0.7 ± 0.1 keV by means of high-resolution elastic-scattering measurements. Unique spin assignments for 15 and parity assignments for 11 resonance levels were obtained. The observed resonance strengths $(2J+1)\Gamma_\gamma\Gamma_p/\Gamma$ vary between 0.077 and 14 eV. Several unusually broad odd-parity resonances were observed which have large reduced widths for p-wave and f-wave capture. The strong contribution of $1f_{7/2}$, $2p_{3/2}$, and $2p_{1/2}$ orbitals to the configuration of states near $E_x=7$ MeV in P^{30} is revealed. The influence of isobaric spin on the level structure and γ-ray decay properties is apparent. The 2^- resonances at $E_p=1470$ and 1686 keV and the 4^- doublet at 1505 keV are identified as T-admixed pairs. Significant revisions of the decay schemes of the 1.45-, 2.94-, 4.14-, 4.50-, and 4.92-MeV levels have resulted from the 40-cc Ge(Li) spectra. The "4.92-MeV level" is shown to be a doublet with components at 4.921 ± 0.002 and 4.945 ± 0.005 MeV. By combining results of the angular-correlation, linear-polarization, and lifetime measurements, the following J^π assignments are derived for bound levels: $0.71(1^+)$, $1.45(2^+)$, $1.97(3^+)$, $2.54(3^+)$, $2.72(2^+)$, $2.84(3^+)$, $2.94(2^+)$, $3.02(1^+)$, $4.14(2^-)$, $4.18(2^+)$, $4.23(4^-)$, $4.43(2^+)$, $4.47(0^+)$, $4.50(1^+)$, $4.62(3^-)$, $4.92(5^-$ or $3^-)$, and $4.94(1)$. Previous $T=1$ assignments for the bound levels at $E_x=0.68$, 2.94, 4.18, 4.47, and 4.50 MeV are strongly supported by the data. Prominent "analog-to-antianalog" $M1$ transitions similar to those in other s-d shell nuclei are observed. An average isospin impurity of 7% for levels below 7 MeV in P^{30} is derived from the set of $E1$ transition rates. On the average, the $E2$ transition rates have strengths slightly less than one Weisskopf unit. However, strong $E2$ enhancement is observed for the $2.94\rightarrow0.68$, $2.54\rightarrow0$, and $2.72\rightarrow0$ transitions which have strengths of 21, 15, and 9 Weisskopf units, respectively. Several of the observed odd-parity resonance and bound levels appear to correspond to $T=1$ and $T=0$ members of a two-nucleon spectrum with major components $(s_{1/2}f_{7/2})$, $(d_{3/2}f_{7/2})$, and $(s_{1/2}p_{3/2})$.

I. INTRODUCTION

IN an earlier paper[1] (hereafter referred to as I), we reported the results of a study of the γ-ray decay schemes of seven resonances between $E_p=700$–1750 keV in the reaction $Si^{29}(p, \gamma)P^{30}$ using large NaI(Tl) detectors and a 2-cc Ge(Li) detector. The decay schemes of the 7 resonances and of 15 bound levels below 5 MeV in P^{30} were presented. Resonance strengths, energies of bound levels with accuracies varying between ±2 and ±4 keV, and a new Q value of 5.597 ± 0.003 MeV for the reaction were also reported.

* Visiting Research Associate under ARL-OSU Research Foundation Contract No. F33615-67-C-1758.
† An element of the Office of Aerospace Research, U. S. Air Force.
[1] G. I. Harris and A. K. Hyder, Jr., Phys. Rev. **157**, 958 (1967).

A more comprehensive extension of the earlier study was considered both possible and desirable. From the experimental standpoint, the availability of a much larger 40-cc Ge(Li) detector, and the use of higher target enrichment and higher average beam currents, made it relatively easy to extend the work to a larger number of resonances. Also, the recognition that the lifetimes of a number of bound levels could be determined in a relatively straightforward manner with large Ge(Li) detectors by Doppler-shift attenuation methods led to an important extension of the work. Apart from the obvious theoretical significance of the lifetimes, they are a considerable aid in making parity assignments in cases where insufficient data are available from other sources. From a more fundamental standpoint, the clear presence of analog-state structure in the resonance region ($E_x \simeq 6$–7 MeV) made it desirable to obtain as much information as possible on a larger selection of resonances. Finally, specific shell-model[2] and collective-model[3] calculations on the lower-lying level structure of P^{30} are now becoming available which add new emphasis to the determination of bound-state spins, parities, lifetimes, and multipolarity mixing ratios.

In this paper, we therefore extend the decay-scheme work in I to include a total of 24 resonances in the region $E_p = 300$–1800 keV ($E_x = 5.9$–7.3 MeV), and present the results of angular-distribution, triple correlation, linear-polarization, and lifetime measurements at many of these resonances. For completeness, the present paper also summarizes the results of a few of the measurements which have been reported briefly elsewhere.[4–6] These previously reported results have now been incorporated in a recent review article.[7] It should be noted that some of the level energies and a Q value reported in this review were taken from a preliminary report,[8] which were superseded by the results reported in I. Other recent work on P^{30} levels includes a study of levels below $E_x = 5$ MeV with the reaction $Si^{28}(He^3, p)P^{30}$ by Vermette *et al.*,[9] lifetime measurements of the 0.678- and 0.709-MeV levels by Kennedy *et al.*,[10] and decay-scheme work with NaI(Tl) detectors on several $Si^{29}(p, \gamma)P^{30}$ resonances by Bergström-Rohlin.[11]

We refrain herein from making a detailed comparison of the results of this work with the results of model calculations in progress elsewhere. For reference, we refer to the earlier shell-model calculations of Glaudemans *et al.*,[12] Wiechers and Brussaard,[13] and Yang Shan-teh[14]; and the calculations by Vermette *et al.*[9] of the mixing ratios and transition probabilities of some of the states of P^{30} predicted by Glaudemans *et al.*[12] Some discussion, however, is presented of possible shell-model configurations of some of the observed odd-parity levels. No discussion of such levels in P^{30} appears to be available elsewhere.

For orientation, the level scheme of P^{30} below $E_x = 5$ MeV and the J^π assignments from the present work are shown in Fig. 1. For comparison, the Si^{30} level scheme is also shown where an arbitrary adjustment has been made to align the Si^{30} ground state and the 0^+, $T=1$ level at 0.678 MeV in P^{30}. The P^{30} level energies are taken from I with the exception of the 0.678-, 2.839-, and 4.945-MeV levels. Recent measurements by Kennedy *et al.*,[10] and in this laboratory, indicate that 0.678 ± 0.001 MeV is better than the value 0.680 ± 0.002 MeV reported in I. The $2.839(\pm 0.010)$-MeV level

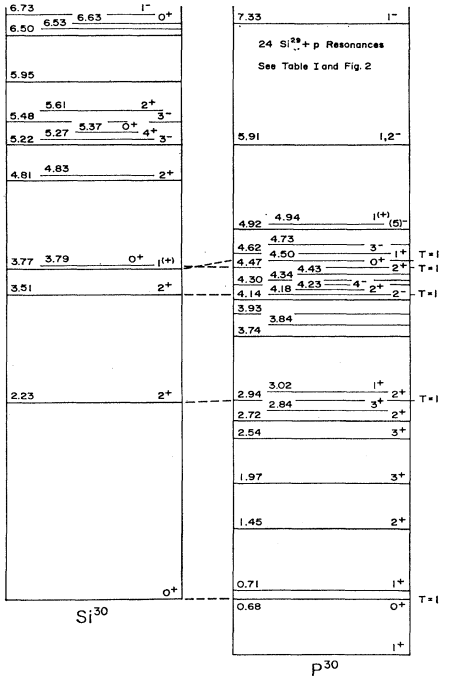

FIG. 1. The low-lying level schemes of Si^{30} and P^{30}. The P^{30} spin and parity assignments, except for the ground-state and 0.678-MeV levels result from the present work. The correspondence between $T=1$ levels is indicated by the dashed lines. The region of excitation energies in P^{30} corresponding to the resonances studied in the $Si^{29}(p, \gamma)P^{30}$ reaction is shown. For additional levels in the region $E_x = 5.0$–5.9 MeV, see Ref. 7.

[2] B. H. Wildenthal, J. B. McGrory, and E. C. Halbert, Phys. Letters **27B**, 611 (1968); and (private communication).
[3] R. J. Ascuitto, D. A. Bell, and J. P. Davidson, Phys. Rev. **176**, 1323 (1968).
[4] G. I. Harris and A. K. Hyder, Jr., Phys. Letters **22**, 159 (1966).
[5] G. I. Harris and A. K. Hyder, Jr., Phys. Letters, **25B**, 210 (1967).
[6] G. I. Harris, in *Nuclear Research with Low Energy Accelerators*, edited by J. B. Marion and D. M. Van Patter (Academic Press Inc., New York, 1967).
[7] P. M. Endt and C. van der Leun, Nucl. Phys. **A105**, 1 (1967).
[8] G. I. Harris and A. K. Hyder, Jr., Bull. Am. Phys. Soc. **12**, 73 (1967).
[9] C. W. Vermette, W. C. Olsen, D. A. Hutcheon, and D. H. Sykes, Nucl. Phys. **A111**, 39 (1968).
[10] E. F. Kennedy, D. H. Youngblood, and A. E. Blaugrund, Phys. Rev. **158**, 897 (1967).
[11] S. Bergström-Rohlin, Arkiv Fysik **35**, 349 (1968).
[12] P. W. M. Glaudemans, G. Wiechers, and P. J. Brussaard, Nucl. Phys. **56**, 529 (1964).
[13] G. Wiechers and P. J. Brussaard, Nucl. Phys. **73**, 604 (1965).
[14] Yang Shan-teh, Acta Phys. Sinica **21**, 1522 (1965).

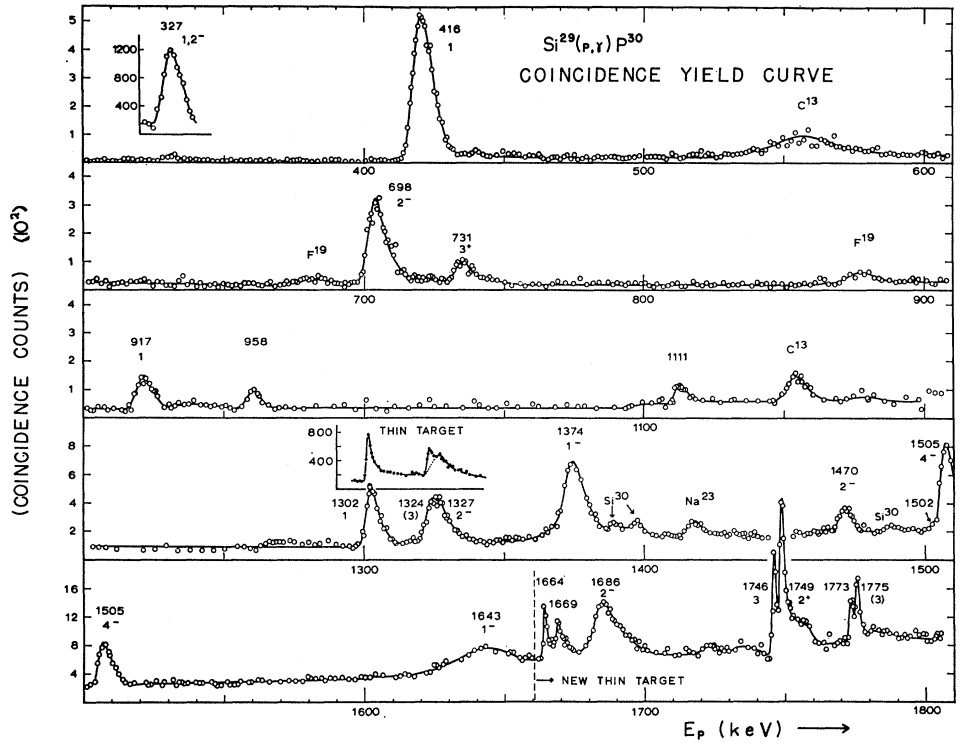

FIG. 2. Coincidence yield curve of the reaction $Si^{29}(p, \gamma)P^{30}$ for $E_p = 300$–1800 keV. The coincidence conditions are given in the text. The resonances due to Si^{29} are labeled by their proton energies (in keV) and J^π assignments resulting from the present work. Resonances due to competing reactions are indicated by the contaminent nuclide. The scale is coincidence counts per 600 μC of protons.

energy is from the reaction $S^{32}(d, \alpha)P^{30}$.[15] The presence of the 4.945-MeV level results from the present work and by comparison with (He^3, $p\gamma$) data.[9] The ground state of P^{30} is known[16] to have $J^\pi = 1^+$ from $P^{30}(\beta^+)Si^{30}$, and the 0.678-MeV level is clearly the 0^+, $T = 1$ analog of the Si^{30} ground state.[15] These values were assumed in the analysis of all the present data which leads to the remaining J^π assignments shown. Earlier assignments are confirmed in many cases.

General comments on the experimental procedure are given in Sec. II. In Secs. III–VII, more specific details of the procedures and analysis are given along with the results of the excitation-curve, decay-scheme, angular correlation, linear-polarization, and lifetime measurements, respectively. The results from the different types of measurements are synthesized and summarized in Sec. VIII. The current "status" of experimental information on P^{30} levels from all known sources is also presented in this section. Section IX contains a discussion and interpretation of results. The results and implications of very recent, high resolution, elastic proton-scattering measurements near $E_p = 1505$ keV are given in the Appendix. The measurements are part of a more extensive elastic-scattering study to be published separately.[17]

[15] P. M. Endt and C. H. Paris, Phys. Rev. **110**, 89 (1958).
[16] G. Morinaga and E. Bleuler, Phys. Rev. **103**, 1423 (1956).
[17] C. P. Poirier, J. Walinga, J. C. Manthuruthil, and G. I. Harris (to be published).

II. GENERAL PROCEDURE

The measurements conducted in the present study consist of the following: (a) the excitation curve for the $Si^{29}(p, \gamma)P^{30}$ reaction in the range $E_p = 300$–1800 keV; (b) γ-ray spectra of 17 resonances in addition to those discussed in I; (c) (p, γ) angular distribution measurements, supplemented in most cases with $(p, \gamma\gamma)$ triple-correlation measurements, at 14 resonances; (d) linear-polarization measurements at 7 resonances; and (e) Doppler-shift-attenuation measurements at 7 resonances. The proton beam was produced by the ARL, 2-MeV Van de Graaff accelerator as discussed in I. In the present work, the targets were prepared in an electron-gun evaporator from SiO_2 [18] with the Si content enriched to 95% Si^{29}. The target material was deposited onto 10-mil-thick Ag backings which, in turn, were soft-soldered onto 0.0625-in.-thick×1.25-in.-diam brass backing plates. The brass-plate target assembly was then mounted on the end of the target chamber in such a way that target cooling could be accomplished by spraying a small stream of distilled water upon the backing plate. No significant deterioration of the targets was observed for typical beam currents of 20–40 μA. The target was mounted at an angle of 45° relative to the proton beam.

[18] The enriched SiO_2 was obtained from the Isotopes Division, Oak Ridge National Laboratory.

The excitation-curve, triple-correlation, and some of the earlier angular-distribution measurements were performed with a combination of 5-in.-diam.×5-in.-long and 8-in.-diam×8-in.-long NaI(Tl) detectors. A commercial (Princeton Gamma-Tech) 40-cc Ge(Li) detector was used for the decay-scheme, later angular-distribution, and lifetime measurements. For most of the work, a 4096-channel analyzer was used to record the data. The data were then stored on magnetic tape which was subsequently processed by an IBM 7094 computer. Additional details of experimental procedure and methods of analysis are given in the sections dealing with the various types of measurements.

III. EXCITATION CURVE, RESONANCE STRENGTHS AND WIDTHS

The excitation curve for the reaction $Si^{29}(p,\gamma)P^{30}$ was measured in the region $E_p=300$–1800 keV [$E_x(P^{30})=5.88$–7.34 MeV] with a setup consisting of an 8×8-in. and a 5×5-in. NaI(Tl) detector. The 8×8-in. detector was mounted with its front face 3 in. from the target spot and at an angle of 55° relative to the proton-beam direction. The 5×5-in. detector was mounted on the opposite side of the target at an angle of 90° relative to the beam and 2 in. from the target. Both singles and coincidence counts were recorded as the beam energy was changed in steps varying in size between about 300 and 3000 eV, depending upon the local structure of the excitation curve. Singles counts were recorded from the 8×8-in. detector which was biased with a low-energy cutoff corresponding to $E_\gamma=2.5$ MeV. Coincidence counts were recorded with the energy conditions $3.5\leq E_\gamma\leq 8.0$ MeV in the 8×8-in. detector and $0.6\leq E_\gamma\leq 3.25$ MeV in the 5×5-in. detector. The resulting coincidence excitation curve is shown in Fig. 2. A similar excitation curve with lower background, but only for selected portions of the region $E_p=1350$–1770 keV, has been given elsewhere.[6]

Most of the data shown were obtained with a relatively thick target (4 keV at $E_p=1.5$ MeV). However a much thinner target was used in regions where preliminary thin-target work had shown the presence of close-lying doublets; i.e., in the region above $E_p=1660$ keV and 1295–1340 keV (see inset). All previously reported resonances were observed except one at $E_p=1727$ keV.[19] In the region $E_p\geq 900$ keV, the results are in good agreement with the lower-resolution work of Moore.[20] For example, the doublets at $E_p=1322$–1327 and 1664–1669 keV first reported by him are confirmed. However, the resonances found by Moore at 1748 and 1772 keV are each shown here to be doublets with components at 1746–1749 and 1773–1775 keV, respectively. (The γ-ray decay scheme reported in I for the 1748-keV "resonance" is thus a combined decay scheme for the two doublet members. The separate decay schemes are given in Sec. IV.) A new weak resonance is identified at $E_p=1502$ keV.[21]

The 1505-keV "resonance" requires special comment. When about all the work discussed in this paper was completed, the 8-MeV ICT Tandem accelerator and associated equipment became available for high-resolution elastic-scattering studies. The first extensive measurements with this accelerator consisted of the measurement of the $Si^{29}(p,p)Si^{29}$ cross section at four angles for $E_p=1100$–2500 keV with a typical resolution of about 200 eV. In this manner it was discovered that the 1505-keV resonance, which had already been studied extensively in proton capture with lower resolution, is a doublet with components separated by only 700 eV. Additional measurements show that the doublet members have nearly identical properties and almost certainly represent a split 4^-, $T=1$ analog state. We have thus chosen to treat this special doublet as a single level throughout the main body of this paper. However, because of the central importance of this resonance to the primary conclusions of this study, we present in the Appendix the necessary data and arguments which justify the treatment as a single level.

No positive evidence is seen in the (p,γ) excitation curve shown for a resonance corresponding to the broad, 1^- ($\Gamma_p=20$ keV) resonance at $E_p=1796$ keV observed here[17] and elsewhere[22,23] in (p,p) scattering data. A weak (p,γ) resonance of this width would, however, have been obscured by the relatively high background encountered in this energy region. Evidence for a weak, broad resonance near this energy has been seen in separate, lower-background runs and also seems to be present in the yield curves of Moore and Bergström-Rohlin. However, neither author mentions its presence. Its existence was confirmed by NaI(Tl) spectra (Sec. IV).

Repeated runs with fresh carbon-free targets were made in the region of the 1746–1749-keV doublet in order to avoid a misinterpretation due to the strong $C^{13}(p,\gamma)N^{14}$ resonance at $E_p=1746$ keV. A similar situation exists at the 1374-keV resonance which is coincident in energy with a $F^{19}(p,\alpha\gamma)O^{16}$ resonance of almost the same width. Positive identification of all resonances was also obtained from γ-ray spectra observed at each resonance in the yield curve. Because of its predominant decay to the ground state (Sec. IV), the 327-keV resonance hardly appears in the coincidence yield curve. Thus we show, as an inset in Fig. 2, a portion of the singles yield curve at this resonance.

The singles yield curve was used to derive the relative

[19] N. K. Green, R. F. Wiseman, and E. A. Milne, Bull. Am. Phys. Soc. **2**, 377 (1957).

[20] R. A. Moore, thesis, University of Kansas, 1963 (unpublished).

[21] This resonance is also reported by S. Bergström-Rohlin (Ref. 11).

[22] V. E. Storizhko and A. I. Popov, Bull, Acad. Sci. USSR Phys. Ser. **28**, 1054 (1965).

[23] A. N. L'vow, A. I. Popov, P. V. Sorokin, and V. E. Storizhko, Bull. Acad. Sci. USSR Phys. Ser. **30**, 447 (1966).

TABLE I. Resonances in the $Si^{29}(p, \gamma)P^{30}$ reaction for $E_p = 300$–1800 keV. The resonance strengths $S = (2J+1)\Gamma_\gamma\Gamma_p/\Gamma$ and the total widths Γ are given. For comparison, resonances reported in Refs. 22 and 23 for $Si^{29}(p, p)Si^{29}$ are also listed. The (p, p) data at 1505 keV is from recent work in this laboratory, to be published elsewhere (Ref. 17).

		$Si^{29}(p, \gamma)P^{30}$		$Si^{29}(p, p)Si^{29}$		
E_p (keV)	$E_x(P^{30})$ (keV)	S (eV)	Γ (keV)	E_p (keV)	Γ (keV)	J^π
327	5.913	0.077±0.015	≤3			
416	5.999	0.70±0.10	≤5			
698	6.272	0.87±0.17	≤4			
731	6.304	0.44±0.09	≤3			
917	6.483	0.40±0.08	≤4			
958	6.523	0.19±0.04	≤2			
1111	6.671	0.21±0.04	≤2			
1302	6.856	1.4±0.3	≤2			
1324	6.877	0.36±0.07	≤2			
1327	6.880	2.4±0.5	5.7±1.0	1331	6	2^-
1374	6.925	4.0±0.8	7.1±0.7	1377	7	1^-
1470	7.018	0.73±0.15	≤4	1470	≤4[a]	$1^-, 2^-$
1502	7.049	(weak)				
1505	7.052	5.0±1.0	≤3	1505[b]	0.037	4^-
1643	7.185	14±3	17.2±2.0	1648	16	1^-
1664	7.206	0.83±0.16	≤1.5			
1669	7.210	0.59±0.12	≤3			
1686	7.227	11±2	5.9±0.7	1686	7	$1^-, 2^-$
1746	7.285	2.2±0.5	≤1.5			
1749	7.288	5.2±1.0	≤2			
1773	7.311	0.87±0.17	≤1.5			
1775	7.313	1.1±0.2	≤1.5			
1792	7.330	≃2.0		1796	20	1^-
				1967	≤3	1^+

[a] Preliminary analysis of (p, p) data obtained in this laboratory shows $\Gamma \simeq 0.5$ keV (Ref. 17).

[b] Doublet with nearly identical members separated by 700 eV. The separate values of Γ, determined in elastic-scattering measurements, are given in the Appendix.

strengths of all $Si^{29}(p, \gamma)P^{30}$ resonances in the manner used in I. As in I, the relative strengths thus obtained were converted to absolute strengths by comparison with the strength $S = (2J+1)\Gamma_\gamma\Gamma_p/\Gamma = 0.70 \pm 0.10$ eV of the $E_p = 416$ keV resonance determined by Engelbertink and Endt.[24] The resonance widths, or upper limits, were extracted from the data of Fig. 2, from that shown in Ref. 6, and from separate measurements not shown. The results, after correction for target thickness and beam energy spread, are given in Table I along with the resonance energies and strengths obtained in this work. For subsequent comparison and discussion, the energies and widths of (p, p) resonances ($E_p \leq 2$ MeV) reported in Refs. 22 and 23 are also listed. Our (p, γ) resonance energies (estimated errors ±2 keV) are in good agreement with other work.[11,19,20] The P^{30} excitation energies E_x are based upon the given resonance energies and the reaction Q value 5.597±0.003 MeV obtained in I. The strength $S = 4.0 \pm 0.8$ eV for the 1374-keV resonance is considerably higher than the preliminary value $S = 1.6$ eV reported earlier.[5] However, the higher value only strengthens the arguments concerning the 4.468-MeV level given in this reference.

IV. RESONANCE DECAY SCHEMES

The spectrum of γ rays from each resonance was obtained with the 40-cc Ge(Li) detector. The detector was mounted with its axis at 55° relative to the incoming beam and approximately $\frac{3}{4}$ in. from the target. Spectra were also obtained at a nearby off-resonance energy in cases where nonresonant background was significant. The targets used for these measurements were typically 3–5 keV thick, except in cases where close-lying doublets were studied with targets of ≃0.5-keV thickness.

The relative intensities of the transitions were derived from relative photopeak, first-, or second-escape peak intensities in the spectra. The intensity calibration of the 40-cc detector is estimated to be accurate to about 15% on a relative basis over the energy range, $1 \leq E_\gamma \leq 8$ MeV, of importance in this study.

The branching ratios in percent of all observed $Si^{29}(p, \gamma)P^{30}$ resonances are collected in Table II. (The J^π assignments given are discussed in following sections.) The results for the 731-, 917-, 1302-, 1470-, 1505-, 1686-keV resonances are generally in good

[24] G. A. P. Engelbertink and P. M. Endt, Nucl. Phys. **88**, 12 (1966).

TABLE II. Branching ratios of the γ decay of $Si^{29}(p,\gamma)P^{30}$ resonances in percent. See text for explanation of values in parentheses.

Resonances		Bound levels of P^{30} (E_x in MeV, J^π)																				
E_p (keV)	J^π	0 1^+	0.68 0^+ $T=1$	0.71 1^+	1.45 2^+	1.97 3^+	2.54 3^+	2.72 2^+	2.84 3^+	2.94 2^+ $T=1$	3.02 1^+	3.74	3.93	4.14 2^-	4.18 2^+ $T=1$	4.23 4^-	4.43 2^+	4.47 0^+ $T=1$	4.50 1^+ $T=1$	4.62 3^-	4.92 $(5)^-$	4.95 $1^{(+)}$
327	$1, 2^-$	82		10	8																	
416	1	4	52	36						3	3							2				
698	2^-	1		2		42	21	25	4		5											
731	3^+	0.6			0.4					80					19							
917	1	6	51		2			2		7					10				22			
958		12		2	16	5	11		14	12					12				(16)			
1111		3					(8)			54					17				(18)			
1302	1	2	76					2		14								6				
1324	(3)				37	17		(9)		29					8							
1327	2^-	73		2	7				3	(3)	6			(6)								
1374	1^-	7	66		9			2										13	3			
1470	2^-	22		9			7				12		(2)	13					33	4		
1502						X^a	X		(X)													
1505[b]	4^-					6	4		4							59				13	14	
1643	1^-	25	11	45							12							3	4			
1664			(3)		5					≥ 80												
1669											≥ 70											
1686	2^-	22		13	6	1	2				4			41						11		
1746	3				25		15			50					10							
1749	2^+	21	2	3	5			18				3					35					13
1773				20		30									20				30			
1775	(3)	5			15	25		5		50												
1792	1^-	X																(X)	X			

[a] The presence of transitions suggested by NaI (Tl) data at the weak 1502- and 1792-keV resonances are indicated by the entry X. The $R \to 0$ transition at the 1792-keV resonance appears about twice as strong as the sum of the transitions to the pair of levels near 4.5 MeV.

[b] Doublet. See Sec. III and the Appendix.

agreement with those reported in I. In a few cases, uncertainty remains about the correct placement of transitions in the decay schemes. In these cases the assignment judged most likely is made, but the branching ratios are enclosed in parentheses. At both the 958- and 1111-keV resonances, the branching to the 4.50-MeV level is uncertain because γ-rays corresponding to the known 4.50→1.45 transition did not appear, although γ rays with correct energies for the R→4.50→0 cascade were present. (R stands for the resonance level.) At the latter resonance, the branch assigned to the 2.54-MeV level could also be assigned as a branch to the 4.14-MeV level. A similar ambiguity about assignments of branches to the 2.72- or 4.14-MeV levels occurs at both the 1324- and 1327-keV resonances. The weak branch to the 2.94-MeV level from the 1327-keV resonance may be due to interference from the strong branch to this level at the neighboring 1324-keV resonance. Several weak transitions not reported previously have been observed.

NaI(Tl) data only were obtained at the weak 1502- and 1792-keV resonances. The transitions which could be identified are indicated in Table II by the entry X. Separate decay schemes were obtained for the 1746- and 1749-keV resonances, whereas in I a combined decay scheme for both resonances was given. The existence of the 4.94-MeV level is deduced from data at the 1749- and 1505-keV resonances (Sec. IV). The branch ratios given for the 1773- and 1775-keV resonances are to be regarded only as approximate because of the difficulty encountered in resolving the two resonances during spectra measurements. The 1664- and 1669-keV resonances are curious in that they decay predominately to the 2.94 ($T=1$) and 3.02 ($T=0$) levels, respectively. This behavior has also been observed by Bergström-Rohlin[11] who, in addition, reported a cascade through a level at 5.50 MeV from the 1669-keV resonance. In general, where comparisons can be made, many changes in decay schemes from those obtained in older, low-resolution NaI work have been necessary. As one example, we note that the 416-keV resonance decays to both levels at 0.68 and 0.71 MeV, where in previous NaI work only a transition to the 0.68-MeV level was assigned.[25,26] The present results are in agreement with recent work with Ge(Li) detectors on this resonance by Kennedy *et al.*[10] The new results suggest a higher degree of isospin mixing in the 416-keV resonance than previously believed.

In I, transitions were observed at the 1302-keV resonance which could only be explained by the presence of a new level of P^{30} at 4.468 MeV. This conclusion was confirmed in the present work by the observation of even stronger transitions involving this new level at the 1374-keV resonance. A weak R→4.468→0 cascade was also observed at the 416-keV resonance.

TABLE III. Revised branching ratios for the decay of the 1.453-, 2.939-, 4.142-, 4.231-, 4.501-, and 4.921-MeV levels of P^{30}. See Ref. 1 for decay schemes of other bound levels. $E_x(i)$ and $E_x(f)$ are the excitation energies of the initial and final levels of the transition, respectively. The results from recent $Si^{28}(He^3, p)P^{30}$ work (Ref. 10) are also shown.

$E_x(i)$ (MeV)	$E_x(f)$ (MeV)	E_γ (MeV)	Relative intensity (%) Present	a
1.453	0	1.453	93±2	95±4
1.453	0.678	0.775	≤2	
1.453	0.709	0.744	7±2	5±4
2.939	0	2.939	17±2	10±6
2.939	0.678	2.261	32±2	43±6
2.939	0.709	2.230	9±2	
2.939	1.453	1.486	42±2	47±6
4.142	0	4.142	72±5	70±4
4.142	0.709	3.433	10±3	14±5
4.142	1.453	2.689	13±3	16±5
4.142	2.939	1.203	5±2	
4.231	0	4.231	4±1	≤10
4.231	1.453	2.778	≤4	12±5
4.231	1.974	2.257	66±3	69±4
4.231	2.536	1.695	27±3	19±4
4.231	2.839	1.392	3±2	
4.501	0	4.501	45±3	42±5
4.501	1.453	3.048	55±3	58±5
4.921	0.678	4.243	≤4	56±7
4.921	0.709	4.212	≤5	
4.921	1.453	3.468	10±3	
4.921	2.939	1.982	≤5	19±3
4.921	4.231	0.690	90±8	25±4

[a] Reference 10.

Although the primary emphasis of the decay-scheme work reported here was to obtain resonance decay schemes based upon bound-state-decay schemes derived in I, it has been necessary to revise the decay schemes of the 1.45-, 2.94-, 4.14-, 4.50-, and 4.92-MeV levels. With the much larger Ge(Li) detector used in the present work, weak 0.744- and 2.230-MeV γ rays were observed during angular-distribution measurements at the 731-keV resonance which could only be explained by the previously unobserved transitions 1.453→0.709 and 2.939→1.453, respectively. The intensities of these weak lines were measured relative to those of the 1.453- and 2.261-MeV transitions from the 1.453- and 2.939-MeV levels, respectively. The new branching ratios which result for the decay of these levels are shown in Table III. From the Table, it can be seen that the results are in reasonable agreement with those from a recent $Si^{28}(He^3, p\gamma)P^{30}$ study[9] in which the γ rays were observed by a 3×3-in. NaI(Tl) detector. The 2.26- and 2.23-MeV γ rays could not, of course, have been resolved in the latter work. The new measurements at the 1470-

[25] C. van der Leun and P. M. Endt. Phys. Rev. **110**, 96 (1958).
[26] E. E. Baart, L. L. Green, and J. C. Willmott, Proc. Phys. Soc. (London) **79**, 237 (1962).

keV resonance yielded branching ratios for the 4.50-MeV level in close agreement with the results of Vermette *et al.*[9] The changes made in the decay scheme of the 4.92-MeV level are discussed below in connection with the angular-correlation measurements at the 1505-keV resonance.

V. ANGULAR CORRELATIONS

A. Procedure and Analysis

The general techniques and methods of analysis used in the angular-distribution (AD) and triple-correlation (TC) measurements have been discussed in previous papers.[6,27–30] Most of the TC measurements have been conducted by techniques which have remained reasonably well standardized. The combination of 8×8-in. and 5×5-in. NaI(Tl) detectors was used in all angular-correlation measurements except in recent measurements where also the 40-cc Ge(Li) detector was used. The finite-geometry correction factors Q_K for the Ge(Li) detector were determined by comparing the angular distributions of selected strong transitions observed by both the 8×8-in. NaI(Tl) and 40-cc Ge(Li) detectors. The Q_K for the NaI(Tl) detector were well known from standard calculations.[28] The asymmetry calibration of the target-detector system was accomplished routinely by measuring the angular distribution of the 2.37-MeV isotropic γ ray from the reaction $C^{12}(p,\gamma)N^{13}$ at $E_p=459$ keV, and in some cases the 7.89-MeV isotropic γ ray at the 620-keV resonance in $Si^{30}(p,\gamma)P^{31}$.

The TC measurements were performed in "geometries" in which two angles of the set $(\theta_1, \theta_2, \varphi)$ were held fixed and the third varied over selected angles between 0° and 90°. In most cases, some or all of the geometries $(\theta_1, \theta_2, \varphi) = (90, V, 180)$, $(V, 90, 180)$, $(90, V, 90)$, and $(V, 90, 90)$ were measured. (The symbol V designates the variable angle of the set.) In a few cases, geometries of the type $(135, V, 180)$ and $(V, 135, 180)$ were used in order to take advantage of the presence, at these fixed angles, of the odd-N terms in the angle function $X_{KM}{}^N(\theta_1, \theta_2, \varphi)$.[30]

The angular correlation of two successive cascade γ rays emitted from an aligned state is given in condensed notation by

$$W(\theta_1, \theta_2, \varphi) = \sum_m P(m) \sum_{KMN} A_{KM}{}^N Q_K Q_M X_{KM}{}^N(\theta_1, \theta_2, \varphi), \quad (1)$$

where the $P(m)$ are the relative populations of the magnetic substates of the emitting state, Q_K and Q_M are finite-geometry correction factors, and $X_{KM}{}^N$ is an angle function. (See, e.g., Ref. 30). The $A_{KM}{}^N$ depend upon the spins of all levels involved in the cascade, and upon the multipolarity mixing ratios δ_1 and δ_2 of the primary and secondary cascade members. The $P(m)$ are defined and normalized such that $P(m) = P(+m) + P(-m)$ and $\Sigma_m P(m) = 1$. Since the spin of Si^{29} and the proton are each $\frac{1}{2}$, only $m=0$ and ± 1 substates are populated at resonance levels formed in the $Si^{29}(p,\gamma)P^{30}$ reaction. Thus we have $P(0)+P(1)=1$ and $P(m\geq 2)=0$. For resonance spins $J_R \geq 2$, alignment is always attained in this reaction. In some cases, the angular correlations of various pairs of transitions in multiple-step cascades were measured. The extension of Eq. (1) to such cases is discussed in Refs. 27, 28, and 30.

The computer programs[28] used for the angular-correlation analysis accept as input data the measured intensity correlations $\bar{W}_a$ at each point a, where a is some fixed combination of the angles θ_1, θ_2, and φ. For each assumed level-spin sequence, the value of the goodness-of-fit parameter χ^2 is computed, where

$$\chi^2 = (1/N) \sum_a (1/\omega_a{}^2)(W_a - \bar{W}_a)^2, \quad (2)$$

for fixed values of $\arctan \delta_1$ and $\arctan \delta_2$. The output format has been described elsewhere,[27,28] Angular distributions are handled by the programs as a special case of the complete angular correlation.

The population parameters $P(m)$ were treated in either of two ways. The $P(m)$ were treated in one version (A) of the basic program as parameters, the best least-squares values of which were computed at each grid point. The condition $P(m) \geq 0$ was imposed as an auxiliary condition. In the other version (B) of the program, the $P(m)$ could be fixed at predetermined values. Version A was always used for the initial analysis of data at any given resonance. Version B was then sometimes used when version A provided a well-defined set of $P(m)$ from the analysis of a specific cascade. This technique was used typically when a resonance decayed through the 0^+ level at 0.678 MeV. The only unknown parameters in such cascades are the resonance spin (J_R) and the $P(m)$. Thus in this case, the $P(m)$ are well determined by the version A analysis for a given value of J_R. The analysis of additional cascades from the same resonance was then done with version B and the $P(m)$ already determined. At other times, this same procedure was used for a quite different reason. It was often found that the correlations were very insensitive to the values of $P(m)$, but at the same time quite sensitive to the mixing ratios δ. Once the insensitivity was verified by version A for all cascades from the resonance, the analysis was repeated using version B and values of the $P(m)$ regarded as most reasonable from consideration of the most likely process of resonance formation.

A resonance can be formed in the $Si^{29}(p,\gamma)P^{30}$

[27] G. I. Harris, H. J. Hennecke, and D. D. Watson, Phys. Rev. **139**, B1113 (1963).
[28] A. K. Hyder, Jr., and D. D. Watson, Aerospace Research Laboratories, Report No. ARL 67-0168, 1967 (unpublished).
[29] G. I. Harris and D. V. Breitenbecher, Phys. Rev. **145**, 866 (1966).
[30] D. D. Watson and G. I. Harris, Nuclear Data **3**, 25 (1967).

reaction either by a unique l value for the incoming proton and a mixture of channel spins $s=0$ and 1, or by a unique channel spin $s=1$ and a mixture of proton orbital momenta. (Neither channel-spin nor orbital momentum mixing would occur in the formation of a $J=0$ resonance.) The relation between the channel-spin mixing parameter t and the $P(m)$, where t is the ratio of formation with $s=1$ to that with $s=0$, is $P(1)/P(0)=t$. In cases where orbital angular-momenta mixing occurs, the relation between the $P(m)$ and the orbital mixing parameter ϵ, where ϵ is the amplitude ratio of completing orbital momenta l and l', is given by[6]

$$P(m)=(1+\epsilon^2)^{-1} \times(C_{J\,lm}{}^2+2f\epsilon C_{J\,lm}C_{J\,l'm}+\epsilon^2 C_{J\,l'm}{}^2), \quad (3)$$

where $C_{J\,lm}=k(lm\ J-m \mid l0)$ and f is the Coulomb phase factor $\cos(\xi_l-\xi_{l'})$. The constant $k=1$ if $m=0$ and $k=\sqrt{2}$ if $m\neq 0$.

It is of value in some cases to convert from the above channel-spin coupling scheme to jj coupling. The channel-spin ratio t is related to the total angular momenta of the proton $j_p=l-\frac{1}{2}$ and $j_p'=l+\frac{1}{2}$ by[6]

$$t=\tfrac{3}{2}(2J_R+1)^{-1}(1+x^2)^{-1}[W^2(l\tfrac{1}{2}J_R\tfrac{1}{2};j_p1) +2xW(l\tfrac{1}{2}J_R\tfrac{1}{2};j_p1)W(l\tfrac{1}{2}J_R\tfrac{1}{2};j_p'1) +x^2W^2(l\tfrac{1}{2}J_R\tfrac{1}{2};j_p'1)], \quad (4)$$

where the amplitude ratio of j_p' to j_p formation is given by x. There are two possible solutions for x because of the quadratic form of Eq. (4). The values of x for the ratio of $p_{3/2}$ to $p_{1/2}$ capture have been obtained from the data at $J^\pi=1^-$ resonances.

Some comment is necessary about the method used in this paper to present and discuss the angular-correlation data. Because of the large amount of data (over 100 angular distributions and 40 triple correlations, each consisting of several geometries) and the analysis routine which uses the observed intensities at each point, a complete presentation of all the data is impractical. The often used method of presenting the coefficients of a Legendre-polynomial fit to the data would not only be uninformative, but also artificial since the analysis does not involve such coefficients. The conclusions are derived instead from an analysis based upon Eqs. (1) and (2) which seeks the best overall fit to the entire set of TC geometries and AD data on a given cascade. In many cases, advantage is taken of the experimental normalization between TC geometries which is not apparent in a Legendre-polynomial representation. In addition, the effect on the TC data of the finite geometry of the detectors is not simply related to the Legendre-polynomial coefficients. Finally, an associated Legendre-polynomial representation would be necessary for many TC results. As a result of these considerations, we have chosen to present the actual data and results of the χ^2 analysis in the form of figures

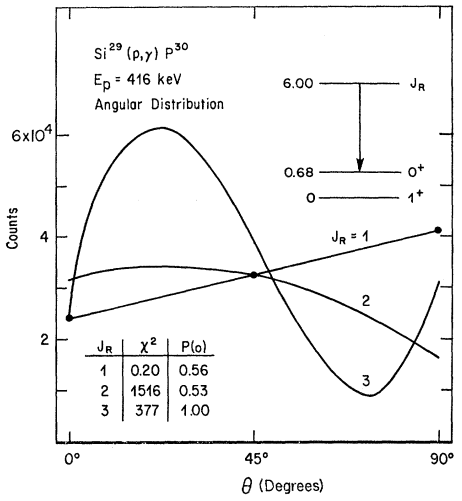

FIG. 3. Angular distribution of the $R\rightarrow 0.678$ transition at the $E_p=416$-keV resonance in $Si^{29}(p, \gamma)P^{30}$. The experimental errors in this case are roughly the size of the dots. The curves, χ^2 values, and $P(0)$ which result from the analysis for different choices of resonances spin J_R are shown. The horizontal scale is linear in $\cos^2\theta$ in all figures of this type. The 0.1% confidence limit is $\chi^2=6.8$ for these data.

in selected cases, and to present the final conclusions for the remaining cases. Final values for J^π and mixing ratios require in many cases a synthesis of data from several sources in addition to the angular correlations. Such synthesis is given in Sec. VIII.

In the following, we assume no prior knowledge of spins of P^{30} levels except $J=1$ and 0, respectively, for $P^{30}(0)$ and $P^{30}(0.678)$. (See Introduction.) The resonance-spin values, population parameters, and multipole mixings which can be deduced from single-step transitions to one or both of these levels are first presented. The information thus obtained is then used as the basis for analysis of cascades which involve other bound levels of P^{30}.

B. Resonance Spins from $R\rightarrow 0$ and $R\rightarrow 0.678$ Transitions

The presence of a $R\rightarrow 0.678$ transition automatically excludes $J_R=0$ and $J_R\geq 4$. $J_R=3$ is also unlikely, but is retained in the analysis. The angular distribution of this transition where it is present leads to a unique value of J_R in all cases. The results of the analysis of a typical case (416-keV resonance) of this type is illustrated in Fig. 3. It is clear that $J_R=1$. In contrast, the angular distributions of $R\rightarrow 0$ transitions do not lead to unique values of J_R because of the additional mixing-ratio parameter δ. However, useful limitations on J_R are obtained. The resonance spins, and the values of $P(0)$ and $\delta(R\rightarrow 0)$ where determined, which result from the analysis of $R\rightarrow 0$ and $R\rightarrow 0.678$ transitions are listed in Table IV. The conservative criterion is used that the χ^2 value must lie above the 0.1% confidence level for the rejection of an assumed spin. The unique values of J_R for the resonances at $E_p=416$, 917, 1302, 1374, 1643,

TABLE IV. Resonance spins J_R and values of $P(0)$ which result from the analysis of angular distributions of $R\rightarrow 0$ and/or $R\rightarrow 0.678$ transitions. The possible values of the $R\rightarrow 0$ multipole-mixing ratio δ are given where determined.

Resonance E_p (keV)	J_R	$\delta(R\rightarrow 0)$	$P(0)$
327	1	$0.34\leq\delta\leq 2.9$ or $-9.5\leq\delta\leq -0.10$	≤ 0.2 or ≥ 0.6
	2	0.03 ± 0.06 or 2.3 ± 0.2	0.4 ± 0.3
416	1	-0.02 ± 0.10 or $\lvert\delta\rvert\geq 8.1$	0.56 ± 0.02
698	1[b]		
	2	-0.18 ± 0.07 or $5.2_{-1.2}^{+3.0}$	0.42 ± 0.06
917[a]	1		0.32 ± 0.05
1302[a]	1		0.33 ± 0.03
1327	1	$0.36\leq\delta\leq 2.7$ or $-7.6\leq\delta\leq -0.13$	≤ 0.19 or ≥ 0.61
	2	0.03 ± 0.06 or 2.3 ± 0.2	0.5 ± 0.3
1374	1		0.94 ± 0.03
1470	1	$0.34\leq\delta\leq 2.9$ or $-9.5\leq\delta\leq -0.10$	≤ 0.21 or ≥ 0.59
	2	0.03 ± 0.07 or 2.4 ± 0.2	0.5 ± 0.3
1643	1	0.00 ± 0.05 or $\lvert\delta\rvert\geq 10$	0.51 ± 0.02
1686	1	$0.33\leq\delta\leq 3.0$ or $-9.5\leq\delta\leq -0.10$	≤ 0.20 or ≥ 0.60
	2	0.03 ± 0.04 or 2.4 ± 0.2	0.5 ± 0.3
1749	2	-0.05 ± 0.04 or 3.5 ± 0.5	0.24 ± 0.09

[a] The angular distributions of all transitions are isotropic at these resonances.

[b] $\delta(R\rightarrow 0)$ and $P(0)$ are undetermined for $J_R=1$.

and 1749 keV result in each case from the $R\rightarrow 0.678$ transition.

C. General Angular Correlations

In this section, an order of discussion is adopted which includes only essential steps and data leading to the conclusions. Those bound levels for which information is obtained by analysis of cascades from resonances listed in Table IV which have unique J_R are considered first. The more complicated cases which occur at resonances with as yet undetermined J_R are then considered. Each discussion is terminated with a brief statement of the general results of the analysis.

416-keV Resonance and the 0.709-MeV Level

A limitation on $J(0.71)$ is obtained from the angular distributions of the $R\rightarrow 0.71$ and $0.71\rightarrow 0$ transitions at the ($J_R=1$) 416-keV resonance. The data and χ^2 projection curves resulting from the simultaneous fit to both angular distributions and with $P(0)=0.56$ are shown in Fig. 4. The values $J(0.71)=0$, 1, 2, and 3 were assumed. The minimum values of χ^2 were 177, 1.16, 3.00, and 19.1, respectively, for each spin choice. The 0.1% confidence limit for these data is $\chi^2=6.8$. Values $J(0.71)\geq 4$ would lead to unreasonable $R\rightarrow 0.71$ transition speeds. We therefore conclude that $J(0.71)=1$ or 2. The $J=2$ possibility is excluded by data at the 1505-keV resonance discussed below. The mixing ratios δ for all transitions are collected in Tables XII and XIII. Conclusion: $J(0.71)=1$.

1374-keV Resonance and the 1.453- and 4.468-MeV Levels

The spin of the 1.45-MeV level is determined uniquely by triple-correlation data on the $R\rightarrow 1.45\rightarrow 0$ cascade at the ($J_R=1$) 1374-keV resonance. The data are shown in Fig. 5 and the χ^2 projection curves for $J(1.45)=2$ in Fig. 6. The minimum values of χ^2 were 188, 36.8, 1.60, and 6.45 for $J(1.45)=0$, 1, 2, and 3, respectively. Since

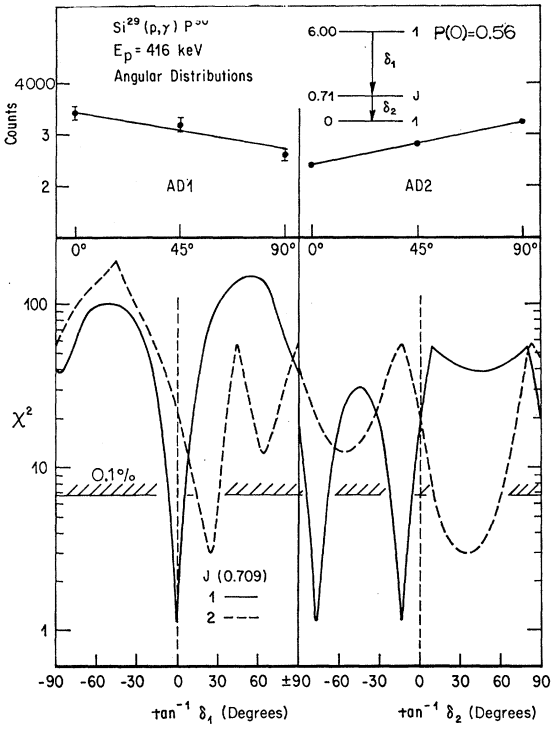

FIG. 4. Angular distributions and χ^2 projection curves for the $R\rightarrow 0.709$ and $0.709\rightarrow 0$ transitions at the 416-keV resonance. Only those χ^2 curves for $J(0.709)=1$ and 2 are shown. Those for $J(0.709)=0$ and 3 were everywhere above the 0.1% confidence level. The lines through the data points are the best fits for $J(0.709)=1$.

the 0.1% confidence level is $\chi^2=3.5$ for these data, the conclusion is $J(1.45)=2$ in agreement with earlier work.[26] The results of angular-correlation and polarization measurements on the $R\rightarrow 4.468\rightarrow 0$ cascade at this resonance have been presented and discussed elsewhere.[5] The analysis of the combined data, not repeated here, showed the resonance to have odd parity and that the 4.468-MeV level is the 0^+, $T=1$ analog of the 3.786-MeV level in Si^{30}. Conclusion: $J(1.453)=2$, $J^\pi(4.468)=0^+$.

1686-keV Resonance and the 4.142-MeV Level

The extensive set of angular-correlation data obtained on the strong $R\rightarrow 4.14\rightarrow 0$ cascade at this resonance has been presented in Ref. 6 and thus not repeated here. The $R\rightarrow 0$ angular distribution yields $J_R=1$ or 2 (Sec. V B). For the choice $J_R=1$, the analysis of the data on the $R\rightarrow 4.14\rightarrow 0$ cascade for $J(4.14)=$ 0, 1, 2, and 3 did not result in an acceptable minimum χ^2. For $J_R=2$, the minimum χ^2 values were 1.10, 0.98, 43.0, and 160 for $J(4.14)=1$, 2, 3, and 4, respectively. Thus, J_R must be 2. $J(4.14)=0$ is excluded by a large observed anisotropy of the $4.14\rightarrow 0$ transition. The final choice $J(4.14)=2$ is made upon the basis of polarization measurements discussed in Sec. VI. Conclusions: $J_R=2$, $P(0)$ undetermined, $J(4.14)=2$.

1505-keV Resonance and the 2.84- and 4.92-MeV Levels

This resonance is remarkable for the amount and uniqueness of information which it provides on P^{30} levels. The results of measurements at this resonance have been reported earlier.[4] This work: consisting of decay-scheme, angular-correlation, and polarization measurements with NaI(Tl) detectors; resulted in the bound-level assignments $0.71(1^+)$, $1.45(2^+)$, $1.97(3^+)$, $2.54(3^+)$, $4.23(4^-)$, $4.62(3^-)$, $4.92(3^-)$, and a resonance

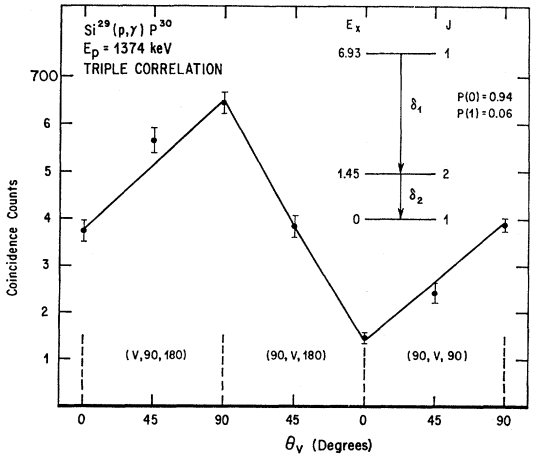

FIG. 5. Triple-correlation data for the $R\rightarrow 1.453\rightarrow 0$ cascade at the 1374-keV resonance. The Geometries are labeled as discussed in Sec. V A of the text. The line through the data points represents the best fit for $J(1.453)=2$.

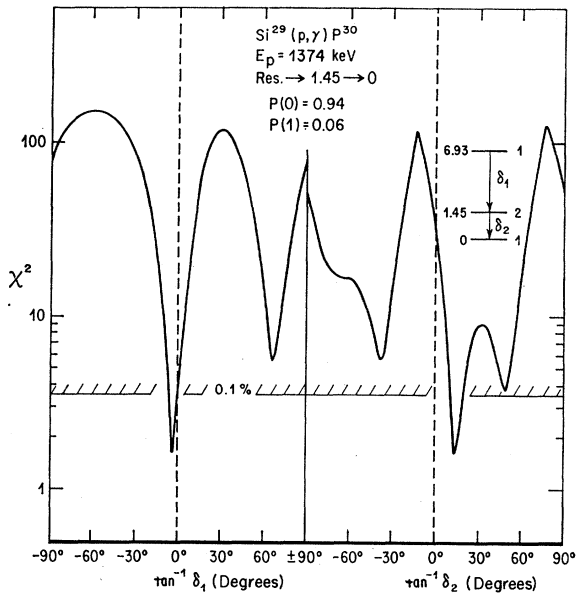

FIG. 6. χ^2 projection curves for the data shown in Fig. 5. The analysis resulted in χ^2 values below the 0.1% confidence level only for the choice $J(1.453)=2$. See text.

assignment of 4^-. Subsequent decay scheme measurements with the 40-cc Ge(Li) detector confirmed most of the NaI(Tl) results, but also revealed previously unobserved weak transitions and required a major revision of the decay scheme of the 4.92-MeV level. (In addition, as mentioned in Sec. III, this resonance was found to be a doublet but is treated here as a single level for reasons discussed in the Appendix.) As a result of the decay-scheme revision, additional angular-correlation measurements have been conducted and all data have been reanalyzed. The earlier level assignments given above were confirmed except that for the 4.92-MeV level. Newly identified cascades through the 2.84-MeV level provided the means to determine its spin.

Rather than to discuss the lengthy analysis in cases where the earlier reported results were confirmed, we present only an example of the angular-correlation data and χ^2 analysis for one of the confirming cases, and discuss in detail the new results or revisions.

The revised resonance decay scheme is shown in Fig. 7. The significant changes involve the 2.839- and 4.921-MeV levels. A 0.694 ± 0.002-MeV γ ray, unrecognized in the earlier data, was observed and identified as a $4.92\rightarrow 4.23$ transition by means of Ge(Li)–NaI(Tl) coincidence spectra. The 4.212-MeV γ ray must be due to a $R\rightarrow 2.839$ transition rather than a $4.921\rightarrow 0.709$ transition; a possibility considered and not entirely excluded in the earlier work.[1,4] The correct placement in the decay scheme of this γ-ray results from Ge(Li)-NaI(Tl) coincidence spectra and consideration of the Doppler shifts obtained during the lifetime measurements (Sec. VII). The spectra show a 1.386-MeV γ ray, in addition to the previously observed 2.13-MeV

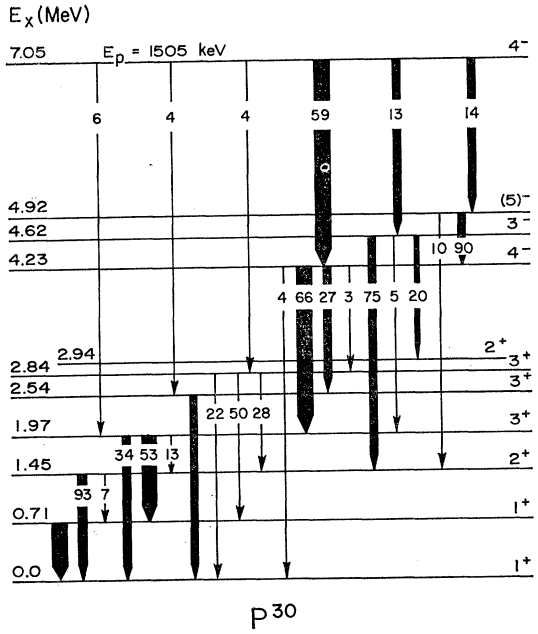

FIG. 7. Decay scheme of the 1505-keV resonance in $Si^{29}(p,\gamma)P^{30}$. The J^π and T assignments result from the present work. The decay of the 2.94-MeV level is not essential to the present discussion and is thus omitted (see Table III). Additional information is given in the Appendix.

γ ray, in coincidence with the 4.21-MeV γ ray. The 1.386-MeV γ ray corresponds to the 2.839→1.453 transition reported by Vermette *et al.*[9] Also the 4.212-MeV γ ray shows a full Doppler shift, indicating that it arises from a short-lived level, whereas the 0.694-MeV γ ray shows only, at most, 20% of the full Doppler shift. Thus, the 4.212-MeV γ ray is not a transition from the 4.921-MeV level. The weak 4.231±0.002 MeV γ ray observed in the spectra is 12±3 keV higher than that expected for a 4.921→0.678 transition, whereas it has exactly the right energy for a 4.231→0 transition. The placement of this γ ray is confirmed by angular-correlation and Doppler-shift measurements. The new branching ratios for the 4.921-MeV level are shown in Table III along with the results of Vermette *et al.*[9] It can be seen that, although the unusual 4.92→4.23 transition is observed in both studies, the branching ratios do not agree. This fact, and the comparison of the angular-correlation results of the two studies, shows that there must be two levels near 4.92 MeV in P^{30}. Both levels must have been simultaneously excited in the $Si^{28}(He^3, p\gamma)P^{30}$ reaction, but only the one which decays predominately to the 4.23-MeV level was excited at the 1505-keV resonance. A level at 4.945-MeV is excited at the 1749-keV resonance (see below).

Figure 8 shows an example from the extensive set of angular-correlation data which confirm, with the exception noted above, the spin assignments reported in Ref. 4. The corresponding χ^2 projection curves are shown in Fig. 9. A small, but statistically significant, $E1$-$M2$ mixing ($\delta = -0.05 \pm 0.02$) results for the $4.23(4^-) \rightarrow 1.97(3^+)$ transition.

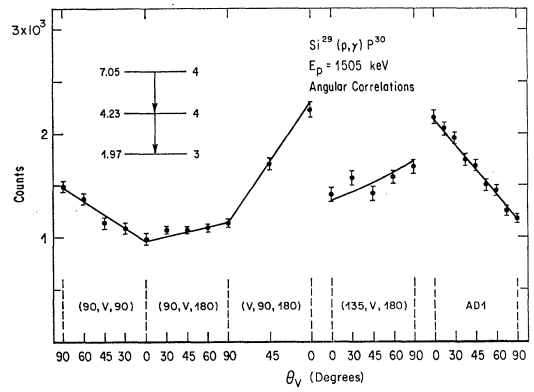

FIG. 8. Angular-correlation data for the $R \rightarrow 4.23 \rightarrow 1.97$ cascade at the 1505-keV resonance. The best fit for the indicated spin assignments is shown.

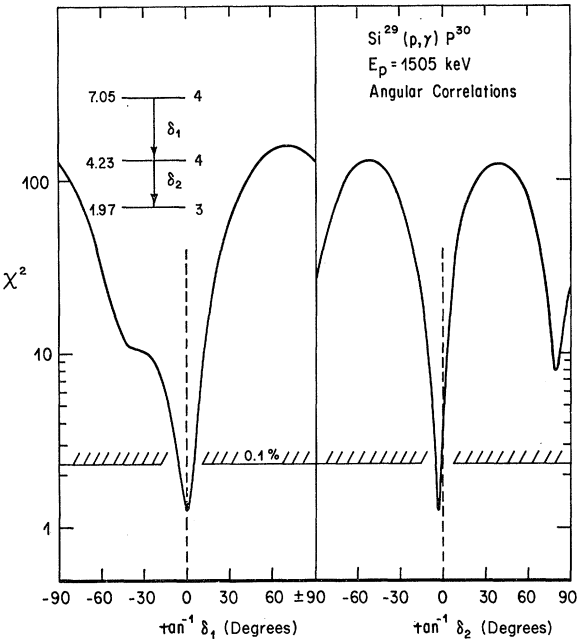

FIG. 9. χ^2 projection curves for the data shown in Fig. 8. The curves shown, for $J(4.23) = 4$, are the only ones which extended below the 0.1% confidence level.

The 2.84-MeV level was shown by Vermette *et al.*[9] to have $J = 1$, 2, or 3. In the present work, the angular distribution of the newly identified $R \rightarrow 2.84$ transition was measured with a Ge(Li) detector. The analysis of this angular distribution for $J(2.84) = 2$, 3, and 4 gave the values $\chi^2 = 38.2$, 0.42, and 3.64, respectively; which are to be compared with a 0.1% level of 5.6. The choice $J(2.84) = 1$ can be eliminated on the basis of the speed of the $R \rightarrow 2.84$ transition derived from the resonance strength. Thus, by comparison with the $Si^{28}(He^3, p\gamma)P^{30}$ data, it can be concluded that $J(2.84) = 3$. For this

assignment, the $R\rightarrow$2.84 mixing ratio is consistent with pure dipole radiation.

As discussed above, the large discrepancy between the branching ratios of the 4.92-MeV level obtained in this work and the (He^3, $p\gamma$) work[9] suggests that the 4.92-MeV level is a doublet. The angular distribution of the 4.92$\rightarrow$0.68 transition observed in the (He^3, $p\gamma$) data yields $J(4.92)=1$. This transition does not appear in the proton-capture spectra at the 1505-keV resonance. As a result of the revision of the decay scheme of the 4.92-MeV level (including the elimination of the earlier assigned 4.92$\rightarrow$0.71 transition, and the addition of the strong 4.92$\rightarrow$4.23 transition), a new series of angular-correlation measurements on cascades which involve this level have been performed. The new decay scheme (Fig. 7) implies, for example, that the possibility $J(4.92)=5$ must now be given serious consideration because of the elimination of the transition to the $J=1$, 0.71-MeV level. The angular correlations measured were as follows:

	Cascade	Geometries
(1)	$R\rightarrow$4.92$\rightarrow$1.45	AD1, AD2, (90, V, 90), (135, V, 180), (V, 90, 180), (90, V, 180)
(2)	4.92$\rightarrow$1.45$\rightarrow$0	AD1, (90, V, 180), (V, 90, 180), (V, 90, 90), (90, V, 90)
(3)	$R\rightarrow$4.92$\rightarrow$4.23	AD1, AD2
(4)	4.92$\rightarrow$4.23$\rightarrow$0	AD1, AD2, (V, 90, 180), (90, V, 180)
(5)	4.92$\rightarrow$4.23$\rightarrow$ 1.97$\rightarrow$0.71	AD1, (V, 90, 180), (90, V, 180).

The angular distributions were obtained with the 40-cc Ge(Li) detector. The angular correlations of cascades (4) and (5) were obtained with the Ge(Li) detector in coincidence with appropriately selected pulses (digital gates selected by an on-line PDP-8 computer) from the 8×8-in. NaI(Tl) detector. The remaining correlations were measured by use of the more conventional NaI-

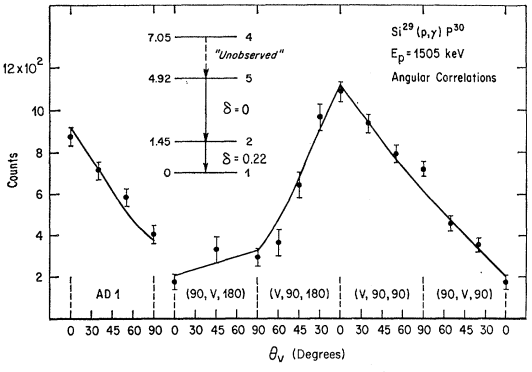

FIG. 10. Angular-correlation data for the 4.92$\rightarrow$1.45$\rightarrow$0 cascade at the 1505-keV resonance. The solid lines are the best fits for $J(4.92)=5$.

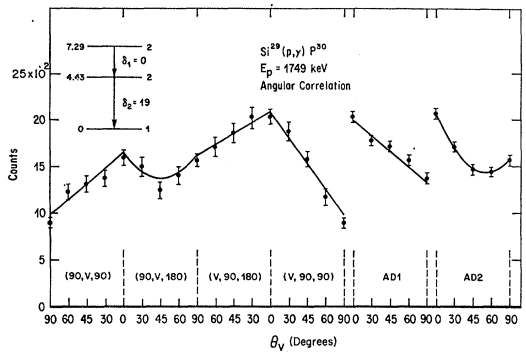

FIG. 11. Combined triple-correlation and angular-distribution data for the $R\rightarrow$4.425$\rightarrow$0 cascade at the 1749-keV resonance. The line through the data points is the best fit for $J_R=J(4.425)=2$. Note the presence of large $P_4(\cos\theta)$ terms caused by the large quadrupole component in the secondary transitions. (See Fig. 12.)

NaI arrangement. [In cascade (5) the 4.23$\rightarrow$1.97 transition was unobserved.]

$J(4.92)=0$ or 1 can be eliminated immediately by consideration of the speed of the $R\rightarrow$4.92 transition derived from the observed resonance strength. The analysis of cascade (3) for the choice $J(4.92)=6$ results in a quadrupole-octupole mixing ($\delta=4.7$) for the $R\rightarrow$4.92 transition. This possibility and higher values of $J(4.92)$ are also eliminated by the transition speed. Thus, $J(4.92)=2$, 3, 4, or 5. For these spins, the analysis of cascade (1) gave the χ^2 values 7.64, 1.33, 1.40, and 1.30, respectively. Thus, $J=2$ is eliminated at the 0.1% level $\chi^2=2.4$ for these data. For $J=3$, 4, and 5, the χ^2 values which resulted from cascade (5) were 1.97, 12.2, and 1.10, respectively. The 0.1% level is 3.4, thus, $J(4.92)=4$ is not possible.

The remaining choice between $J(4.92)=3$ or 5 is much more difficult. Upon analysis of preliminary data and a detailed consideration fo the correlations to be expected in various geometries, it was found that only cascade (2) could possibly distinguish between the two spins. Thus a series of angular-correlation measurements were conducted on the rather weak 4.92$\rightarrow$1.45$\rightarrow$0 cascade. The measurements were made possible by the fact that the weak 3.468 MeV, 4.92$\rightarrow$1.45 transition is higher in energy than the intense transitions of this resonance. In the analysis, the population parameters of the 4.92-MeV level were chosen to correspond to the values of $\delta(R\rightarrow 4.92)$ obtained from cascades (1) and (3) and to f-wave resonance formation. [The resonance is known to have odd-parity from the polarization results discussed in Sec. VI, and the (p, p) data discussed in the Appendix.] The values of $\delta(R\rightarrow 4.92)$ and $P(m)$ were varied to establish that the correlations were insensitive to these parameters over reasonable ranges. We also have available the results that the 4.92-MeV level has odd parity whether $J(4.92)=3$ or 5, and that the 1.45-MeV level has even parity. (See Sec. VI.) Thus, if $J(4.92)=5$, the 4.92$\rightarrow$1.45 transition would be $E3$. It is therefore reasonable

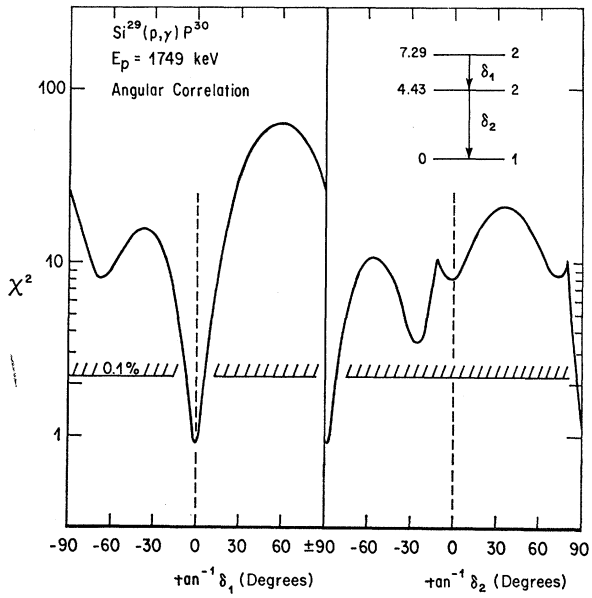

FIG. 12. χ^2 projection curves for the data shown in Fig. 11. The curves shown are those which resulted in the lowest χ^2 values of all spin combinations tested.

to assume no mixing in this transition for the choice $J=5$.

The data are shown in Fig. 10. It can be seen from the figure that the fit to the data is good ($\chi^2=1.40$) for $J(4.92)=5$ and $\delta(1.45\rightarrow 0)=0.22$ in agreement with values obtained at other resonances, and for pure octupole radiation for the 4.92→1.45 transition. The fit for $J(4.92)=3$ is just as good ($\chi^2=1.35$) for the same $\delta(1.45\rightarrow 0)$. However, for this assignment we find that the 4.92→1.45 transition must have $\delta=-0.73\pm0.07$ which, because of the parity change, corresponds to mixed $E1$-$M2$ radiation. Such a high $E1$-$M2$ mixing would be extremely unusual. This fact, coupled with considerations of transition speeds discussed in following sections, strongly favors the $J=5$ assignment to the 4.92-MeV level. Conclusions: $J(2.84)=3$ and $J(4.92)=5$ or 3.

1749-keV Resonance and the 4.425- and 4.945-MeV Levels

The set of angular correlation data for the $R\rightarrow 4.43\rightarrow 0$ cascade at this resonance is shown in Fig. 11. It can be seen that strong $P_4(\cos\theta)$ terms appear in AD2 and the geometry (90, V, 180) triple correlation. Thus one can conclude immediately that J_R and $J(4.43)\geq 2$. We already have $J_R=2$ from the $R\rightarrow 0.68$ angular distribution (Table IV). These preliminary conclusions were verified by the complete χ^2 analysis of the data of Fig. 11. The data were analyzed for all combinations of $J_R=1$, 2, and 3 with $J(4.43)=0$, 1, 2, 3, and 4 subject to the constraints $|\Delta J|\leq 2$ in the primary transition and $|\Delta J|\leq 3$ in the secondary transition. $J_R=0$ and ± 4 are excluded by the presence of the transition $R\rightarrow 0.68$.

The only combination which resulted in χ^2 values below the 0.1% level ($\chi^2=2.2$ for these data) was $J_R=J(4.43)=2$. The χ^2 projection curves are shown in Fig. 12. It can be seen that the 4.43→0 transition is predominately quadrupole ($\delta_2=-19_{-10}^{+5}$), while the $R\rightarrow 4.43$ transition is pure dipole ($\delta_1=-0.01\pm0.03$).

An argument given in I based upon transition-energy measurements that the assumed $R\rightarrow 4.43\rightarrow 0$ cascade was not a possible inverted $R\rightarrow 2.84\rightarrow 0$ cascade was confirmed by an analysis of the correlation data of Fig. 11, in which the inverted order was assumed. For all reasonable choices J_R and $J(2.84)$, no value of χ^2 below the 0.1% confidence level was obtained. In addition, it has been shown by Vermette *et al.*[9] that the 2.84-MeV level decays predominately (50%) to the 0.71-MeV level. The corresponding 2.13-MeV γ ray has not been observed at the 1749-keV resonance. The possibility of a dipole-quadrupole-octupole admixture in the 4.43→0 transition has also been investigated. This analysis was done by means of an appropriate modification of the H_M term and the single-parameter method of angular-correlation analysis described in Ref. 27. Although several solutions were found, all except the one equivalent to the solution shown in Fig. 12 (essentially pure quadrupole) led to unreasonably high $E2$ or $M3$ transition speeds when combined with the 4.43-MeV-level lifetime result given in Sec. VII.

Two γ rays appear in the spectra at this resonance which have almost exactly the correct energies for a $R\rightarrow 3.02\rightarrow 0.68$ cascade, and they were assigned as such in I. However, the angular distributions of these two γ rays could not be fitted for any choice of $\delta(R\rightarrow 3.02)$ and the known level spins. (The 3.02-MeV level has $J=1$ as discussed below in connection with the 1470-keV resonance.) Since the angular distributions of these γ rays were derived from Ge(Li) spectra yielding consistent angular distributions of several other transitions, it is clear that the decay-scheme assignment is incorrect. The only reasonable alternative is to invert the order of the two transitions in question. The

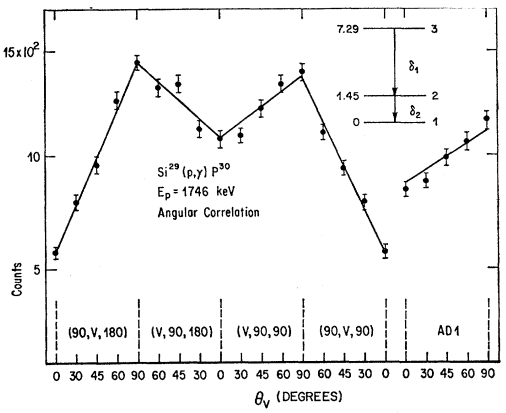

FIG. 13. Combined triple-correlation and angular-distribution data for the $R\rightarrow 1.453\rightarrow 0$ cascade at the 1746-keV resonance. The line is the best fit for $J_R=3$.

energies are such that the inverted order would correspond to a $R \rightarrow 4.945 \rightarrow 0.68$ cascade. A level of this energy could be a member of the expected doublet near 4.92 MeV (see discussion above of the 1505-keV resonance). With this decay-scheme assignment, the analysis of the angular distribution yields a good fit for the spin sequence $2 \rightarrow 1 \rightarrow 0$. The χ^2 values for $J(4.945)=1$, 2, and 3 were 1.20, 4.35, and 15.0, respectively. Thus $J=1$, in agreement with the result for the "4.92-MeV level" obtained by Vermette *et al.*[9] from the angular distribution of the $4.94 \rightarrow 0.68$ transition in the $Si^{28}(He^3, p\gamma)P^{30}$ reaction. The decay-scheme assignment $R \rightarrow 4.94 \rightarrow 0.68$ has also been suggested recently by Bergström-Rohlin.[11] Conclusions: $J_R=2$, $P(0)=0.24\pm0.09$, $J(4.425)=2$, and $J(4.945)=1$.

1746-keV Resonance

The spin of this resonance is determined uniquely by angular-correlation measurements on the $R \rightarrow 1.45 \rightarrow 0$ cascade. The result $J(1.45)=2$ obtained at the 1374-keV resonance is assumed. The data are shown in Fig. 13 and the results of the χ^2 analysis in Fig. 14. The minimum χ^2 values were 3.60, 11.6, 1.18, and 19.8 for $J_R=1$, 2, 3, and 4, respectively. ($J_R=0$ is eliminated by the anisotropic angular distributions, and $J_R \geq 5$ would lead to unreasonably fast transitions.) Only $J_R=3$ is acceptable at the 0.1% confidence level $\chi^2=2.5$. The value $\delta(1.45 \rightarrow 0)=0.15\pm0.04$ is not in good agreement with the value 0.25 ± 0.03 obtained at the 1374-keV resonance. However, the values of this mixing ratio obtained with other choices of J_R are in much worse

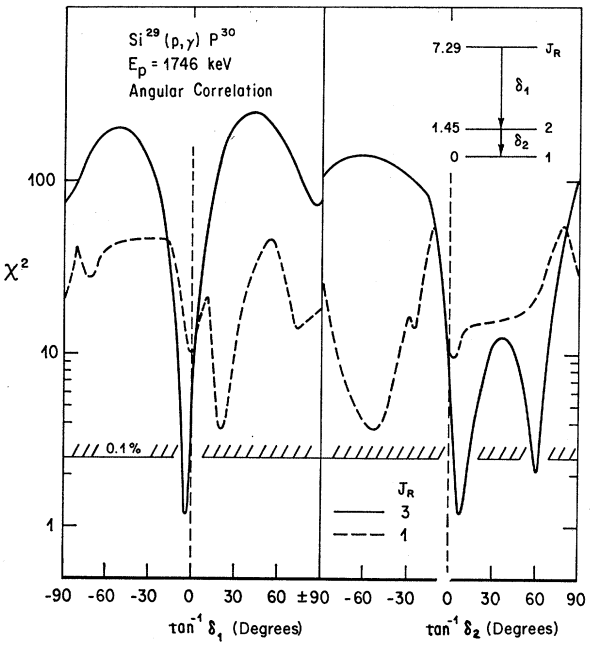

FIG. 14. χ^2 projection curves for the data shown in Fig. 13. The minimum χ^2 values for choices of J_R not shown are higher than those shown.

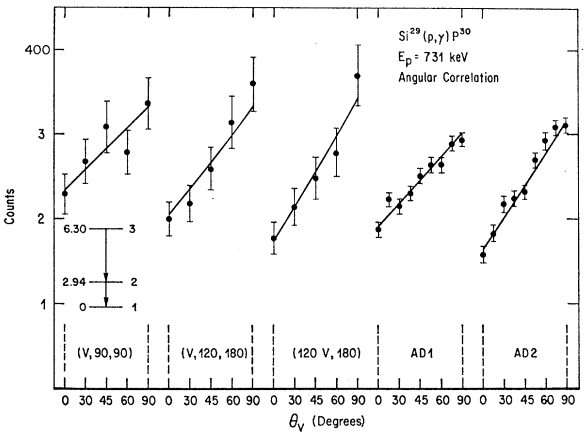

FIG. 15. Angular-correlation data for the $R \rightarrow 2.94 \rightarrow 0$ cascade at the 731-keV resonance.

agreement. The discrepancy is believed to be caused by incomplete experimental resolution of the 1746- and 1749-keV resonances. The 1749-keV resonance also has a weak decay branch to the 1.45-MeV level. Conclusions: $J_R=3$, $P(0)=0.33\pm0.07$.

731-keV Resonance and the 2.939- and 4.182-MeV Levels

We first consider the resonance and 2.94-MeV levels. The analysis is simplified considerably by taking note of a nonzero $P_4(\cos\theta)$ term observed in a NaI(Tl) angular distribution of the unresolved $2.939 \rightarrow 0.678$ and $2.939 \rightarrow 0.709$ transitions. The observed distribution was $W=1+(0.39\pm0.02)P_2-(0.17\pm0.03)P_4$ in excellent agreement with the result $W=1+(0.38\pm0.08)P_2-(0.18\pm0.04)P_4$ obtained by Baart *et al.*[26] Thus both levels have spin of 2 or greater. The spin of the 2.94-MeV level is further limited to values $J \leq 3$ by the presence of the $2.94 \rightarrow 0.68(0^+)$ transition.

The angular-correlation data obtained for the $R \rightarrow 2.94 \rightarrow 0$ cascade are shown in Fig. 15. The analysis was conducted for all combinations of $J_R=2$, 3, 4, and $J(2.94)=2$, 3; and resulted in the unique solution $J_R=3$, $J(2.94)=2$. The χ^2 projection curves for this case are shown in Fig. 16.

The angular distributions of the two members of the $2.94 \rightarrow 1.45 \rightarrow 0$ cascade were measured with the Ge(Li) detector for the primary purpose of obtaining the mixing ratio of the $2.94 \rightarrow 1.45$ transition. The unique results $\delta(2.94 \rightarrow 1.45)=0.03\pm0.03$ and $\delta(1.45 \rightarrow 0)=0.29\pm0.07$ were obtained. The latter value is in good agreement with the value $\delta=0.25\pm0.03$ obtained at the 1374-keV resonance.

A series of angular-correlation measurements similar to that shown in Fig. 15 was obtained on the $R \rightarrow 4.18 \rightarrow 0.71$ cascade. These data were analyzed for $J(4.18)=0$, 1, 2, 3, 4; and the values $J_R=3$, $J(0.71)=1$ already established. All values except $J(4.18)=2$ were eliminated at the 0.1% confidence level. The mixing ratios

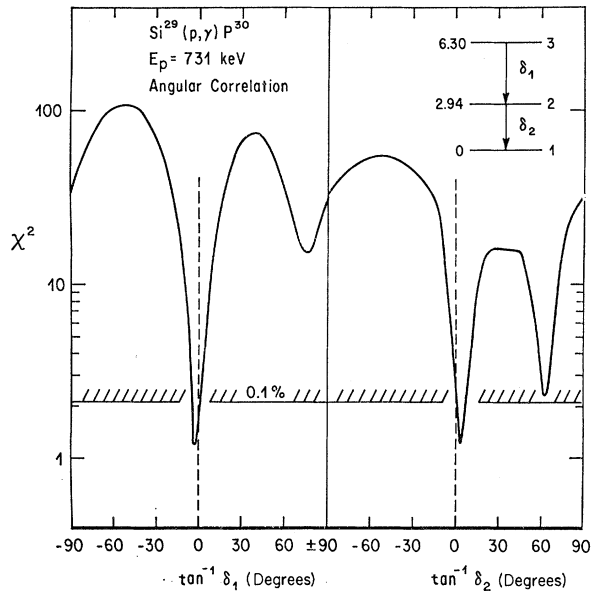

FIG. 16. χ^2 projection curves for the data shown in Fig. 15.

obtained for the primary and secondary transitions are consistent with pure dipole radiations. Conclusions: $J_R=3$, $P(0)=0.5\pm0.2$, $J(2.939)=2$, $J(4.182)=2$.

1470-keV Resonance and the 3.020- and 4.501-MeV Levels

The resonance spin, already limited to $J_R=1$ or 2 by the $R\rightarrow0$ angular distribution (Sec. V B), is determined uniquely by a set of angular-correlation data on the $R\rightarrow0.71\rightarrow0$ cascade. The data (not shown) included 4 triple-correlation geometries and the $R\rightarrow0.71$ angular distribution obtained with the 40-cc Ge(Li) detector. The analysis gave $\chi^2=1.20$ for $J_R=2$ and 4.69 for $J_R=1$. The 0.1% level is $\chi=2.8$. For $J_R=2$, the value of $\delta(R\rightarrow0.71)$ is consistent with pure dipole radiation, the values of $\delta(0.71\rightarrow0)$ are consistent with values obtained at other resonances, and $P(0)=0.44\pm0.04$ for the resonance level.

The 3.02-MeV level was found to have $J=1$, in agreement with earlier results,[9,26] by means of an extensive set of angular correlations on the $R\rightarrow3.02\rightarrow0.68\rightarrow0$ cascade at this resonance. The mixing ratio for the $R\rightarrow3.02$ transition is consistent with pure dipole radiation.

The analysis associated with the 4.50-MeV level is discussed in more detail. This level has been assumed[1] to be the $J=1$, $T=1$ analog of the 3.77-MeV level of Si^{30}, although no unique spin assignment has been previously obtained.

Angular distributions of all members, and triple correlations between all pairs of members, of the triple cascade $R\rightarrow4.50\rightarrow1.45\rightarrow0$ were measured. The analysis was conducted as follows: First, the data for the cascade $R\rightarrow4.50\rightarrow1.45$ were analyzed for the known values of J_R and $J(1.45)$, and for $J(4.50)=0$ through 4. [The $R\rightarrow4.50$ transition speed rules out higher values of $J(4.50)$.] The resultant χ^2 values were 50.1, 0.81, 0.93, 1.15, and 3.13 for $J(4.50)=0$, 1, 2, 3, and 4, respectively. Thus, $J=0$ and 4 are eliminated at the 0.1% confidence level, $\chi^2=2.9$. $J(4.50)=4$ is additionally excluded by the high value $\delta=11.5$ obtained in this case for the $R\rightarrow4.50$ transition, which implies an octupole transition rate inconsistent with the known transition speed. Next, the angular correlations between the first and third members of the cascade were analyzed for the known spins and $J(4.50)=1$, 2, and 3. Here the values of $\delta(4.50\rightarrow1.45)$ were varied over ranges consistent with the results from the $R\rightarrow4.50\rightarrow1.45$ analysis. The data are shown in Fig. 17. For $J(4.50)=1$, 2, and 3, the minimum values of χ^2 obtained were 0.80, 4.63, and 1.02, respectively. Thus, $J=2$ is excluded. Finally, the data (Fig. 17) for the $4.50\rightarrow1.45\rightarrow0$ cascade were analyzed for $J(4.50)=1$, 2, and 3 for values of the population parameters of the 4.50-MeV level consistent with the results of the above analysis. For $J=1$, 2, and 3, the χ^2 values were 0.89, 7.42, and 3.4, respectively. Thus, $J=4$ is again clearly excluded, and $J=3$ yields a χ^2 value slightly above the 0.1% level, $\chi^2=3.2$. The $J=3$ assignment was eliminated more positively by computing the weighted averages of the χ^2 projection curves for the transitions which were common in the three sets of angular correlations. (The weighting

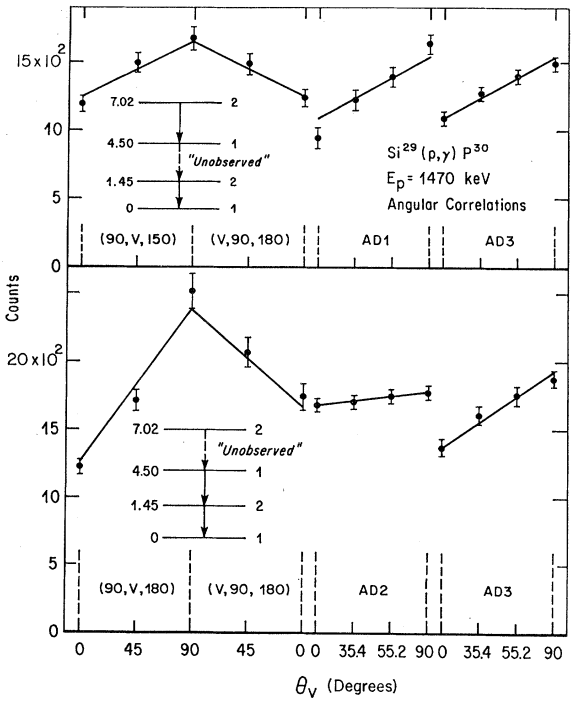

FIG. 17. Angular-correlation data for the $R\rightarrow4.50\rightarrow1.45\rightarrow0$ triple cascade at the 1470-keV resonance. The upper portion shows data for the correlation of the first and third members of the cascade, and the lower portion shows those for the second and third members. The lines represent the best fits for $J(4.50)=1$.

factors were given by the numbers of degrees of freedom.) the resultant average χ^2 curve for the 4.50→1.45 transition had a minimum of 35.3 for values of $\delta(1.45\rightarrow 0)$ in the region of the value already determined at other resonances. Thus, $J(4.50)=1$. The weighted average χ^2 curves for this assignment are shown in Fig. 18. The mixing ratios for the first two transitions are consistent with pure dipole radiation, and the smaller of the two ratios obtained for the 1.45→0 transition is in good agreement with that previously determined. Conclusions: $J_R=2$, $P(0)=0.44\pm0.04$, $J(3.02)=1$, and $J(4.50)=1$.

698-keV Resonance and the 2.722-MeV Level

The previous assignment[26] of $J_R=2$ was confirmed by measurement of the angular distributions [Ge(Li) detector] of the members of the $R\rightarrow1.97\rightarrow0$ cascade. The results $J(1.97)=3$, established at the 1505-keV resonance, and $J_R=1$ or 2 (Table IV) were assumed in the analysis. The angular distributions of the members of the $R\rightarrow2.54\rightarrow0$ cascade were in close agreement with the results of Baart *et al.*,[26] but yield no information on the 2.54-MeV level in addition to that already available from the data at the 1505-keV resonance.

The angular distributions of the members of the $R\rightarrow2.72\rightarrow0$ cascade are shown in the upper part of

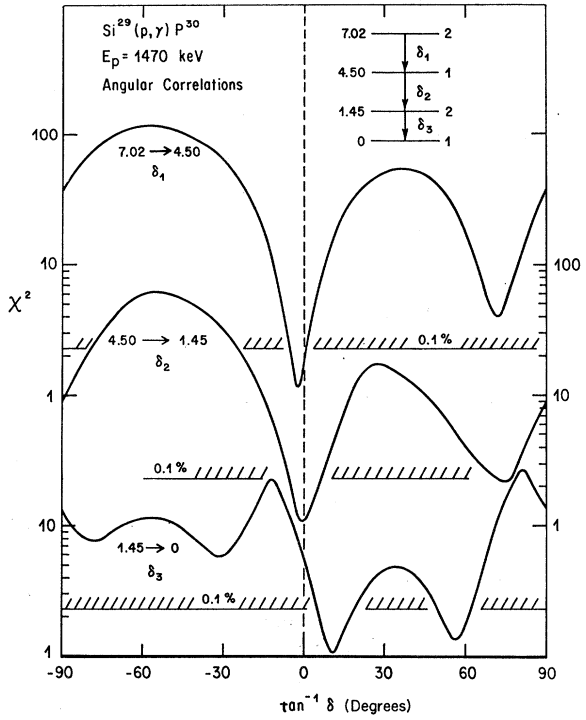

FIG. 18. χ^2 projection curves for the three members of the $R\rightarrow4.50\rightarrow1.45\rightarrow0$ cascade at the 1470-keV resonance. Each curve is the weighted average of curves for common transitions in the three sets of angular-correlation data on this cascade. See text. The scales on the left refer to the curves of δ_1 and δ_3, while the scale on the right refers to the δ_2 curve.

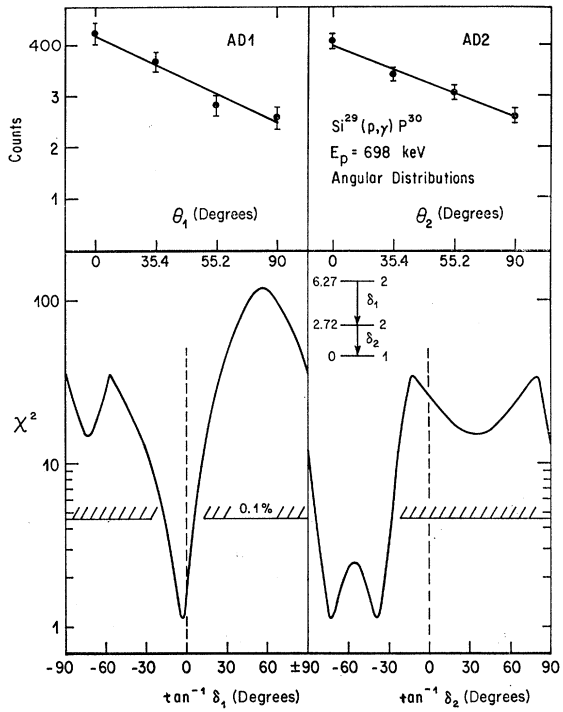

FIG. 19. Angular-distribution data and χ^2 projection curves for the $R\rightarrow2.72\rightarrow0$ cascade at the $E_p=698$-keV resonance. The lines through the data points and the χ^2 curves are for the most probable assignment $J=2$ for the 2.72-MeV level.

Fig. 19. For $J_R=2$ and values of $P(0)$ consistent with those determined from the $R\rightarrow1.97\rightarrow0$ cascade [$P(0)=0.42\pm0.06$], the minimum $\chi^2_{\frac{1}{2}}$ values for these data were all near 1.2 for $J(2.72)=1$ to 4, respectively. $J(2.72)=0$ is excluded by the anisotropy of AD2. The values of $\delta(2.72\rightarrow0)$ which correspond to the assignments $J(2.72)=1$, 2, and 3 are given in Table VI where they are considered in relation to polarization measurements. The $J(2.72)=4$ possibility can be excluded by consideration of the resonance strength and the observed $\delta(R\rightarrow2.72)$. An $E3$ strength of at least 4×10^3 Weisskopf units, and even higher for $M3$, is implied by this assignment. No choice can be made between the remaining spin possibilities without the additional information available from the polarization and lifetime data. The χ^2 projection curves for the assignment $J(2.72)=2$ resulting from this additional information are shown in the lower part of Fig. 19. The solution $\delta(2.72\rightarrow0)=-3.3_{-0.6}{}^{+0.8}$ is in rough agreement with the most probable value $-11_{-6}{}^{+\infty}$ reported by Vermette *et al.*[9] A value $\delta(2.72\rightarrow0)=-0.7$ (after correction for the difference in sign convention) was reported by Baart *et al.*[26] However, an independent analysis of their data reveals another solution in the neighborhood of the high value obtained by Vermette *et al.*, and in the present work. It thus appears most likely that the 2.72-MeV level decays to the ground state predominately by quadrupole radiation. Conclusions: $J_R=2$, $P(0)=0.42\pm0.06$, $J(2.72)=2$.

1322-keV Resonance

Angular distributions of the transitions $R\rightarrow 1.97$, $R\rightarrow 2.94$, $2.94\rightarrow 0.68$, and $2.94\rightarrow 1.45$ were measured at this resonance with the 40-cc Ge(Li) detector. The essential considerations which lead to the probable assignment $J_R=3$ are as follows: $J_R=0$ is excluded by anisotropic angular distributions, and $J_R\geq 5$ by transition speeds derived from the observed resonance strength. The analysis of the $R\rightarrow 1.97$ angular distribution for $J_R=1$ [and the result $J(1.97)=3$ determined above at the 1505-keV resonance] yields $|\delta|(R\rightarrow 1.97)\geq 0.14$. This value corresponds to an octupole ($E3$) transition speed of at least 280 Weisskopf units—an unreasonably high value. This same angular distribution is consistent with either $J_R=2$ or 3. $J_R=4$ is excluded by the value $\chi^2=16.0$ obtained from the analysis of the two members of the $R\rightarrow 2.94\rightarrow 1.45$ cascade using the previously determined spins $J=2$ for the 2.94- and 1.45-MeV levels. For $J_R=2$ and 3, the χ^2 values obtained for the $R\rightarrow 2.94\rightarrow 0.68$ cascade were 3.3 and 1.6, respectively. While both values are below the 0.1% confidence level, $\chi^2=5.0$ for the data, the latter is a factor of 10 more probable on a statistical basis. The mixing ratios obtained for the $R\rightarrow 2.94$ transition are $\delta=0.58\pm 0.12$ and -0.03 ± 0.05, for $J_R=2$ and 3, respectively. The former value is not typical of primary transitions observed at other resonances in this reaction. $J_R=3$ is in good agreement with all the data. Conclusions: $J_R=3$ (2 not rigorously excluded), $P(0)$ undetermined.

1773- and 1775-keV Resonances

The first indication of the existence of a doublet instead of a single resonance near $E_p=1772$ keV came from the analysis of sets of triple-correlation data on the $R\rightarrow 1.97\rightarrow 0$ and $R\rightarrow 2.94\rightarrow 0.68$ cascades. The two sets of data gave different resonance spins. Later yield-curve measurements with very thin targets revealed directly the two resonances (Fig. 2). It was then found that the 2.94-MeV level appears to be excited only at the higher-energy resonance, while both resonances decay to the 1.97-MeV level (Table II). Thus no reliable information was obtained from the $R\rightarrow 1.97\rightarrow 0$ triple-correlation data or, as a consequence, on the spin of the 1773-keV resonance. However the $R\rightarrow 2.94\rightarrow 0$ data do provide information on the 1775-keV resonance. The data (not shown) consisted of the three mutually normalized triple-correlation geometries (V, 90, 180), (90, V, 180), and (90, V, 90). The minimum values of χ^2 for $J_R=1$, 2, 3, and 4 were 1.54, 4.28, 0.93, and 2.19, respectively; to be compared with the 0.1% level $\chi^2=2.8$. Thus, $J_R=2$ is excluded. $J_R=0$ and ≥ 5 lead to unreasonable transition speeds. For $J_R=4$, the $R\rightarrow$ 2.94 transition must be mixed quadrupole-octupole ($\delta=0.25\pm 0.05$) which also leads to an unreasonably high octupole transition speed. Thus, $J_R=1$ or 3. $J_R=3$ is to be preferred over $J_R=1$ because of the prominent transition to the $J=3$, 1.97-MeV level (Table II). For $J_R=3$, we have $\delta(R\rightarrow 2.94)=-0.23\pm 0.05$. Conclusions: $J_R(1773)$ undetermined. $J_R(1775)=1$ or 3, probably 3; $P(0)(1775)=0.44\pm 0.05$ if $J_R=3$.

VI. LINEAR POLARIZATIONS

A. Procedure and Analysis

Details of the linear polarization methods used in this study are published elsewhere.[6,30–32] The experimental polarization

$$P_{\text{expt}}=(1/p)[(N_\perp-N_{||})/(N_\perp+N_{||})] \qquad (5)$$

was determined with a Compton polarimeter for 28 transitions which appear at the resonances at $E_p=698$, 731, 1374, 1470, 1505, and 1686 keV. $N_{||}$ and $N_\perp$ are the number of Compton-scattered quanta observed by a detector located in the plane defined by the emitted γ ray and the proton-beam axis, and by a detector located perpendicular to this plane, respectively. The polarimeter efficiency p for the apparatus used in this work has been tabulated for $1\leq E_\gamma\leq 5$ MeV by Willmes and Harris.[31] The tabulated efficiencies have, however, been multiplied by the factor $(1-2\beta)=0.878$ discussed by Lee and Watson,[32] which approximates the effect of the finite azimuthal extent of the analyzing detectors.

The analyzing detectors were two 5×5-in. NaI(Tl) crystals mounted at a relative azimuthal angle of 90°, which observed the radiation scattered from a 2×2-in. NaI(Tl) crystal located with its axis on a line extending vertically from the target. The entire polarimeter could be rotated about this vertical axis in order to reduce the effects of polarimeter asymmetries by interchanging effectively the roles of the two analyzing detectors. The coincidence pulses from the two scattering-crystal, analyzing-crystal combinations were summed electronically[32] and routed to separate memory subgroups of the multichannel analyzer. The resulting coincidence spectra were subsequently analyzed by spectrum stripping procedures[33] discussed and illustrated in I.

The theoretical polarization with which Eq. (5) is to be compared is given by

$$P(\theta)=\pm[W(\theta)]^{-1}\sum_m P(m)\sum_\nu B_{\nu m}P_\nu^2(\cos\theta), \qquad (6)$$

where the plus sign is used if there is no parity change in the transition, and the minus sign is used if there is a parity change. (In the present work, $\theta=90°$.) The calculation of $B_{\nu m}$ using tabulated coefficients is discussed in Ref. 30. $W(\theta)$ is the angular distribution of the observed transition. The results are discussed below for all except the 1374-keV resonance which has been discussed previously.[5]

[31] H. Willmes and G. I. Harris, Phys. Rev. **162**, 1027 (1967).
[32] F. D. Lee and D. D. Watson, Nucl. Instr. Methods **61**, 328 (1968).
[33] H. D. Graber and D. D. Watson, Nucl. Instr. Methods **43**, 355 (1966).

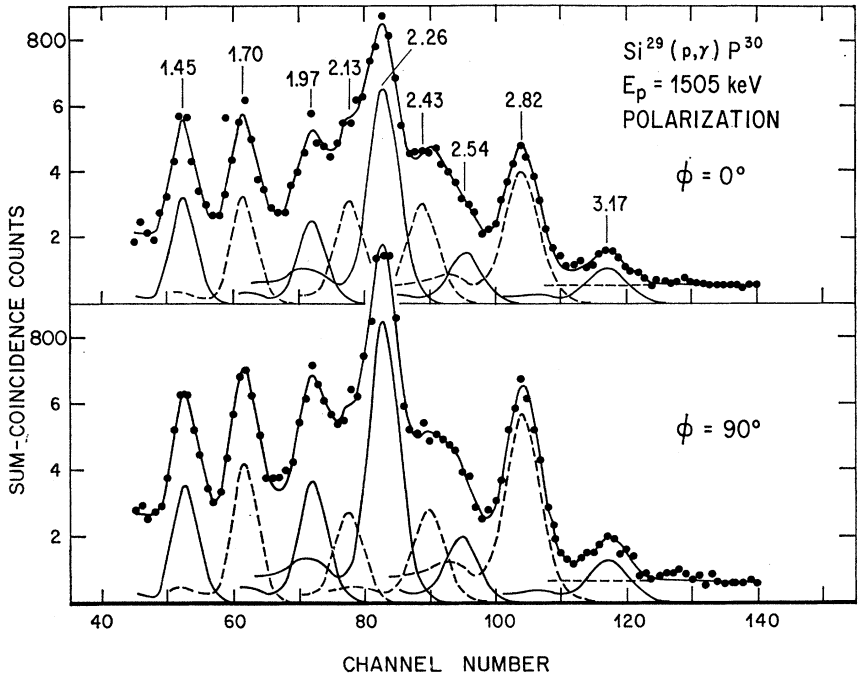

FIG. 20. Linear-polarization data obtained with a Compton polarimeter at the 1505-keV resonance in $Si^{29}(p, \gamma)P^{30}$. The γ-ray energies are indicated in MeV. See Fig. 7 for their placement in the decay scheme. The spectrum labeled $\phi=0°$ corresponds to the detection of the Compton scattered radiation in the plane defined by the proton beam and the emitted γ-rays, and the spectrum $\phi=90°$ corresponds to detection in a direction perpendicular to this plane. The line through the data points represents the best fit obtained by the spectrum stripping program.

B. Polarization Results

1505-keV Resonance and the 0.71-, 1.97-, 2.54-, 4.23, 4.62-, and 4.92-MeV Levels

One of the three sets of polarization data obtained at the 1505-keV resonance is shown in Fig. 20. The three sets yielded consistent results although the one shown was the most accurate because of better statistics and electronic alignment. The spectra, although complex at this resonance, were analyzed satisfactorily by the spectrum-stripping program using empirical polarimeter line shapes obtained from a series of separate measurements with radioactive sources and (p, γ) reactions producing relatively isolated γ-ray lines of various energies. The results were found to be relatively insensitive to slight variations in the line shapes by reanalysis with altered line widths and tail heights. The various components of the spectrum are shown in Fig. 20 along with the fitted curve through the data points, which represents the sum of the separate components. The over-all fit is seen to be very good.

The relative intensity given by the fitting program for the corresponding components of the two spectra were used to compute the experimental polarization of each transition according to Eq. (5). The results are given in Table V. The polarizations of the 5.08- and 1.27-MeV

TABLE V. Linear-polarization results at the 1505-keV resonance in $Si^{29}(p, \gamma)P^{30}$. P_{expt} and P_{theor} are the experimental and theoretical polarization, respectively. The two columns under P_{theor} correspond to the cases in which the lowest-order radiation in the transition is electric or magnetic, respectively.

Transition	E_γ (MeV)	$J_i \to J_f$	$P_{theor}(EL)$	$P_{theor}(ML)$	P_{expt}	Radiation type
$R \to 1.97$	5.08	$4 \to 3$	0.42	−0.42	0.56±0.51	$E1$
$R \to 4.23$	2.82	$4 \to 4$	−0.89	0.89	0.76±0.19	$M1$
$R \to 4.62$	2.43	$4 \to 3$	0.42	−0.42	−0.61±0.28	$M1$
$R \to 4.92$	2.13	$4 \to 3$	0.42	−0.42	−0.44±0.22	$M1$
		$4 \to 5$	0.28	−0.28	−0.44±0.22	$M1$
$1.97 \to 0$	1.97	$3 \to 1^+$	0.68	−0.68	0.82±0.22	$E2$
$1.97 \to 0.71$	1.26	$3 \to 1$	0.68	−0.68	0.52±0.17	$E2$
$2.54 \to 0$	2.54	$3 \to 1^+$	0.68	−0.68	0.47±0.33	$E2$
		$4 \to 1^+$	−0.90	0.90	0.47±0.33	$M3$
$4.23 \to 1.97$	2.26	$4 \to 3$	0.37	−0.37	0.43±0.14	$E1$
$4.23 \to 2.54$	1.70	$4 \to 3$	0.37	−0.37	0.42±0.21	$E1$
		$4 \to 4$	−0.16	0.16	0.42±0.21	$M1$
$4.63 \to 1.45$	3.17	$3 \to 2$	0.42	−0.42	0.33±0.30	$E1$

TABLE VI. Linear-polarization results at the 698-keV resonance. The symbols δ_1 and δ_2 refer to the multipolarity mixings, obtained from the angular correlation, of the primary and secondary radiations of the cascade considered.

Transition	$J_i \to J_f$	δ_1	δ_2	$P_{\text{theor}}(EL)$	$P_{\text{theor}}(ML)$	P_{expt}	Radiation type
$R \to 1.97$	$2 \to 3^+$	0.05	...	0.18	−0.18	0.44±0.22	*E*1-*M*2
1.97→0	$3 \to 1^+$	0.05	0.0	0.63	−0.63	0.53±0.18	*E*2
1.97→0.71	$3 \to 1^+$	0.05	0.0	0.63	−0.63	0.37±0.14	*E*2
2.54→0	$3 \to 1^+$	0.08	0.0	0.63	−0.63	0.63±0.18	*E*2
2.72→0	$1 \to 1^+$	−0.51	−0.44 or −2.3	−0.05	0.05	0.08±0.14	*E*1-*M*2[a]
2.72→0	$1 \to 1^+$	−9.5	0.72 or 1.4	0.59	−0.59	0.08±0.14	
2.72→0	$2 \to 1^+$	−0.04	−0.78	0.24	−0.24	0.08±0.14	*E*1-*M*2
2.72→0	$2 \to 1^+$	−0.04	−3.3	−0.03	0.03	0.08±0.14	
2.72→0	$3 \to 1^+$	0.84	−0.20	0.38	−0.38	0.08±0.14	
2.72→0	$3 \to 1^+$	0.84	−23.	0.54	−0.54	0.08±0.14	

[a] The choice of radiation type depends in this case upon the value of δ_1 and the resonance strength (see text).

γ rays were obtained from other spectra not shown. This Table also lists the values of the theoretical polarizations P_{theor} to be expected for the two transition types and the spins and mixing ratios already determined from the angular-correlation data. The conclusion regarding the radiation type is given in the last column of the Table. Uncertainties in P_{theor} due to the uncertainties in the relevant mixing ratios, branching ratios, and resonance population parameters are much smaller than the error in P_{expt}; so they are not given. The P_{theor} are given for each of the two values $J(2.54)=3$ and 4 which remain from the angular-correlation analysis.

By reference to Table V and the decay scheme (Fig. 7), the parities of the resonance and six bound levels of P^{30} are easily deduced using the well-known γ-ray selection rules and the initial assumption $J^\pi(0)=1^+$. The spin *and* parity of the 2.54-MeV level are fixed by the polarization data as follows: The parity of the 4.23-MeV level is odd as can be deduced from the polarizations of the 4.23→1.97 and 1.97→0 transitions. Assume $J(2.54)=4$. The polarization of the 4.23→2.54 transition then requires odd parity for the 2.54-MeV level. However, this result is contradicted by the observed polarization of the 2.54→0 transition which would require even parity. On the other hand, the polarization results are consistent with $J^\pi(2.54)=3^+$. Conclusions: $J^\pi(R)=4^-$ and the bound-state spin-parity assignments; $0.71(1^+)$, $1.45(2^+)$, $1.97(3^+)$, $2.54(3^+)$, $4.23(4^-)$, $4.62(3^-)$, and $4.92(5^-$ or $3^-)$.

698-keV Resonance and the 2.72-MeV Level

The polarizations of five transitions at the 698-keV resonance were derived from a set of data similar to that shown in Fig. 20, but with poorer statistics because of the lower resonance strength. The results are presented in Table VI. It can be seen that the even-parity assignments obtained above for the 1.97- and 2.54-MeV levels are confirmed. Odd parity is required for the resonance by the polarization of the $R \to 1.97$ transition.

The polarization of the 2.72→0 transition is compared in the table with the values which correspond to the various solutions remaining from the angular-correlation analysis at this resonance (Sec. V). Limitations on the possible solutions are imposed by the 2.72→0 polarization and the resonance strength. For $J(2.72)=3$, the most likely solution is for $P_{\text{theor}}=0.38$, which differs by more than two standard deviations from the observed value 0.08±0.14. This solution would imply that the $R \to 2.72$ transition is mixed *E*1-*M*2 with $\delta=0.84$, which leads to an unreasonably high *M*2 speed of 220 Weisskopf units.[34] The case in which $J(2.72)=1$ and $\delta(R \to 2.72)=-9.5$ leads to a discrepancy of almost 4 standard deviations between P_{expt} and P_{theor}. The solution $J(2.72)=1$ and $\delta(R \to 2.72)=-0.51$ yields agreement with the polarization data for either type of radiation. The resonance strength and $\delta(R \to 2.72)$ imply, in this case, odd parity for the 2.72-MeV level. The 2.72→0 transition would thus be mixed *E*1-*M*2 as indicated in the Table. Similar considerations for the $J(2.72)=2$ solutions results in the limitations $J^\pi(2.72)=2^-$ and $\delta(2.72 \to 0)=-0.78$, or $J^\pi(2.72)=2^+$ or 2^- and $\delta(2.72 \to 0)=-3.3$. The final choice for $J^\pi(2.72)$ results from the lifetime measurements discussed in Sec. VIII. Conclusions: $J^\pi(R)=2^-$; $J^\pi(2.72)=1^-$, 2^+, or 2^-.

731-keV Resonance and the 2.94- and 4.18-MeV Levels

The polarization data obtained at this resonance are shown in Table VII. The two members of the 2.94→

[34] S. J. Skorka, J. Hertel, and T. W. Retz-Schmidt, Nucl. Data 2, 347 (1966).

TABLE VII. Linear-polarization results at the 731-keV resonance.

Transition	E_γ (MeV)	J_i-J_f	$P_{\text{theor}}(EL)$	$P_{\text{theor}}(ML)$	P_{expt}	Radiation type
$R\rightarrow 2.94$	3.37	$3\rightarrow 2$	0.45	−0.45	-0.31 ± 0.14	$M1$
$R\rightarrow 4.18$	2.12	$3\rightarrow 2$	0.45	−0.45	-0.29 ± 0.25	$M1$
$1.45\rightarrow 0$	1.45	$2^+\rightarrow 1^+$	0.13	−0.13	0.23 ± 0.10	$M1$-$E2$
$2.94\rightarrow 1.45$	1.49	$2\rightarrow 2^+$	−0.64	0.64		$M1$

1.45→0 cascade were not resolved in the polarimeter spectra. However, their combined polarization is easily computed from the values in the Table for the separate polarizations to be $P_{\text{theor}}=0.26$ or -0.39 for $J^\pi(2.94)=2^+$ or 2^-, respectively. The observed value $P_{\text{expt}}=0.23\pm0.10$ thus fixes the parity of the 2.94-MeV level as even. The polarization of the $R\rightarrow 2.94$ transition then requires that the resonance have even parity. (A small correction has been applied to P_{expt} for $R\rightarrow 2.94$ for the effect of the unresolved 4.18→0.71 transition.) Finally, the even-parity resonance assignment and the value of P_{expt} for $R\rightarrow 4.18$ yields even parity for the 4.18-MeV level. The resulting 2^+ assignments for the 2.94- and 4.18-MeV levels is in accordance with their previous assignment[15] as the $T=1$ analogs of the first and second excited states of Si^{30}. Conclusions: $J^\pi(R)=3^+$, $J^\pi(2.94)=2^+$, and $J^\pi(4.18)=2^+$.

1686-keV Resonance and the 4.142-MeV Level

The polarizations of the members of the $R\rightarrow 4.14\rightarrow 0$ cascade were measured at this resonance with good precision because of the high resonance strength and relatively simple γ-ray spectrum. The results are compared in Table VIII with the polarizations expected for the solutions for $J(4.14)$, $\delta(R\rightarrow 4.14)$, and $\delta(4.14\rightarrow 0)$ which remain from the angular-correlation analysis (Sec. V C). By inspection, it is seen that if $J(4.14)=1$, then the $R\rightarrow 4.14$ transition must be mixed $E1$-$M2$ with $\delta=-0.49$. The resulting $M2$ transition speed would be 4.3×10^3 Weisskopf units—an unreasonably high value. The polarization of the 4.14→0 transition is also not in agreement in magnitude with the expected values for this solution. Thus, $J(4.14)=2$. For this spin assignment, there remain two possible solutions: either $R(2^-)\rightarrow 4.14(2^-)\rightarrow 0(1^+)$ with $\delta_1=-0.02$ and $\delta_2=0.01$, or $R(2^+)\rightarrow 4.14(2^+)\rightarrow 0(1^+)$ with $\delta_1=-0.02$ and $\delta_2=2.54$. No definite choice between these solutions can be made with available proton-capture data. However, the resonance has been shown elsewhere[22] to have odd parity by elastic proton-scattering measurements. Conclusions: $J^\pi(R)=2^-$, $J^\pi(4.14)=2^-$.

1470-keV Resonance and the 3.02- and 4.50-MeV Levels

At this relatively weak resonance, the polarizations of only a few of the strongest low-energy transitions were extracted reliably from the data. In Table IX, we see that the $R\rightarrow 4.14$ polarization, when combined with the $J^\pi(4.14)=2^-$ assignment obtained above, fixes the resonance parity as odd, in agreement with the elastic-scattering data.[22] The values of P_{expt} for the $R\rightarrow 4.50$ transition, which includes a small correction for the effect of the weak unresolved 2.54→0 transition at this resonance (see I), shows that the 4.50-MeV level has even parity. The 1^+ assignment for the 4.50-MeV level is in accordance with its earlier assignment[1,15] as the $T=1$ analog of the 3.77-MeV level of Si^{30}. The 3.02→0.68 polarization yields even parity for the 3.02-MeV level. Conclusions: $J^\pi(R)=2^-$, $J^\pi(3.02)=1^+$, and $J^\pi(4.50)=1^+$.

VII. LIFETIME MEASUREMENTS

A. Procedure and Analysis

The techniques used here are very similar to those described by Wolff *et al.*[35] The primary difference is our use of the phenomenological approach to the energy

TABLE VIII. Linear-polarization results at the 1686-keV resonance.

Transition	$J_i\rightarrow J_f$	δ_1	δ_2	$P_{\text{theor}}(EL)$	$P_{\text{theor}}(ML)$	P_{expt}	Radiation type
$R\rightarrow 4.14$	$2\rightarrow 1$	−0.49	...	0.82	−0.82	0.75 ± 0.12	$E1+M2$
$R\rightarrow 4.14$	$2\rightarrow 1$	−19	...	−0.40	0.40	0.75 ± 0.12	
$R\rightarrow 4.14$	$2\rightarrow 2$	−0.02	...	−0.64	0.64	0.75 ± 0.12	$M1+E2$
$4.14\rightarrow 0$	$1\rightarrow 1^+$	−0.49	1.0	−0.65	0.65	0.21 ± 0.12	
$4.14\rightarrow 0$	$2\rightarrow 1^+$	−0.02	0.01	0.15	−0.15	0.21 ± 0.12	$E1+M2$
$4.14\rightarrow 0$	$2\rightarrow 1^+$	−0.02	2.54	−0.24	0.24	0.21 ± 0.12	$M1+E2$

[35] A. C. Wolff, M. A. Meyer, and P. M. Endt. Nucl. Phys. **A107**, 332 (1968).

TABLE IX. Linear-polarization results at the 1470-keV resonance.

Transition	E_γ (MeV)	$J_i \to J_f$	$P_{\text{theor}}(EL)$	$P_{\text{theor}}(ML)$	P_{expt}	Radiation type
$R \to 4.14$	2.88	$2 \to 2^-$	−0.64	0.64	0.60±0.35	$M1$
$R \to 4.50$	2.52	$2 \to 1$	0.45	−0.45	0.37±0.14	$E1$
$3.02 \to 0.68$	2.34	$1 \to 0^+$	0.45	−0.45	−0.26±0.18	$M1$
$4.50 \to 1.45$	3.05	$1 \to 2^+$	0.05	−0.05	−0.27±0.25	

loss and scattering of the recoil ions discussed by Warburton *et al.*,[36] instead of the theory elaborated by Blaugrund.[37] The equivalence of the two approaches has been demonstrated by Warburton *et al.*

The γ-ray energies at 6 resonances between $E_p=0.7$ and 1.75 MeV were measured with the 40-cc Ge(Li) detector at the angles θ_1 and θ_2 with respect to the proton beam. The measurements at the two angles were alternated in many short (10-min) runs as a means of reducing the effect of gain drift. Relatively thick targets ($\simeq$15 keV for 1.5-MeV protons) were used to insure that the recoiling P^{30} ions stopped completely in the target layer. The angles used were $\theta_1=0°$ and $\theta_2=120°$ or 130° except in one case (1374-keV resonance) where $\theta_1=30°$ and $\theta_2=120°$ had to be used because of very strong angular distributions of some of the γ rays of interest.

From the measured energy shifts $\Delta E_\gamma = E_\gamma(\theta_1) - E_\gamma(\theta_2)$, the quantity

$$F(\tau) = [\Delta E_\gamma / E_{\gamma 0} \beta(0) (\cos\theta_1 - \cos\theta_2)] \qquad (7)$$

was computed, where $E_{\gamma 0}$ is the γ-ray energy which would result from emission by the nucleus at rest and $\beta(0)=v(0)/c$ is the initial recoil velocity of the P^{30} ions. The attenuation coefficient $F(\tau)$ $[0 \leq F(\tau) \leq 1]$ is the ratio of the observed shift to that which would occur for lifetimes very short compared to the stopping time.

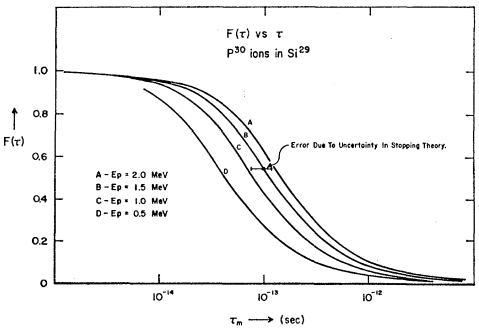

FIG. 21. The Doppler shift F, expressed as a fraction of the full shift, as a function of the mean life, for P^{30} ions stopping in Si^{29}.

[36] E. K. Warburton, J. W. Olness, and A. R. Poletti, Phys. Rev. 160, 938 (1967).

[37] A. E. Blaugrund, Nucl. Phys. 88, 501 (1966).

Where possible, the Doppler shift was determined from both the photopeaks and second-escape peaks in the spectra. The peak centroid positions were obtained by a computer program with a Gaussian fitting procedure.

The attenuation factor $F(\tau)$ is related to the mean life τ and the electronic and nuclear stopping parameters K_e and K_n by the expression[36]

$$F(\tau) = x\gamma^x (1+\gamma^2)^{-(1/2)x} \int_0^1 V^2 (\gamma^{-2}+V^2)^{(1/2)x-1} dV, \qquad (8)$$

where $x=\alpha_e/\tau$, $\gamma = 137(K_e/K_n)^{1/2}\beta(0)$ and $\alpha_e = M_1 c/137\rho K_e$. M_1 is the mass of the moving ion. The evaluation of K_e and K_n and their uncertainties are discussed by Warburton *et al.*

Curves of $F(\tau)$ versus τ were computed by numerical integration of Eq. (8) for values of α_e and γ of interest

TABLE X. Lifetime measurements of bound states of P^{30}.

E_x (MeV)	E_p (keV)	Decay to (E_x in MeV)	$F(\%)$ [a]	τ_m (10^{-15} sec)	$\langle\tau_m\rangle_{\text{av}}$ [b] (10^{-15} sec)
1.45	1374	0	10±9	≥240	≥240
1.97	698	0	3±8	≥240	≥240
		0.71	6±9		
2.54	698	0	36±5	92±21	92±21
2.72	698	0	38±5	84±17	96±15
	1748	0	50±6	126±27	
2.94	731	0.68	64±8		
				32±6	
		1.45	72±7		37±5
	1746	1.45	79±4	47±9	
4.14	1686	0	74±6	58±14	58±14
4.23	1505	0	0±3		
		1.97	7±5	≥1200	≥1200
		2.54	0±5		
4.42	1749	0	72±3	64±8	64±8
4.47	1374	0	98±8	≤33	≤33
4.62	1505	1.45	31±8	220±90	260±60
	1686	1.45	30±10	290±70	
		2.94	27±7		
4.92	1505	1.45	2±5	≥800	≥800
		4.23	0±8		
4.94	1749	0.68	79±9	47±20	47±20

[a] Some values are average shifts of the full-energy and double-escape peaks.

[b] The upper (lower) limits correspond to the average measured value of F minus (plus) 2 times the standard deviation.

to this work. The curves which result for selected proton energies between 0.5 and 2.0 MeV are shown in Fig. 21. An exact knowledge of the Si-SiO_2 ratio in the target is not necessary since the Doppler-shift attenuation for Si and SiO_2 are the same with 2%.[35] The quoted errors for τ correspond to the uncertainty of the $F(\tau)$ from the data. Possible errors in the slowing-down theory are not included. (See, however, Fig. 21).

B. Lifetime Results

The measurements were performed at the resonances at $E_p=698$, 731, 1374, 1505, 1686, 1746, and 1749 keV. For each level in question, the Doppler shifts were obtained at resonances at which the level is strongly excited directly from the resonance. Corrections for the very short resonance lifetimes were unnecessary. In some cases, the lifetime of a given level could be determined from two or more transitions from the level, or from measurements at different resonances. The observed attenuation factor F and the corresponding lifetimes for 12 levels of P^{30} are shown in Table X. The source resonance is indicated in each case. It can be seen that the values of F obtained from different transitions from the same level are in good agreement, as also are the lifetimes derived from data at different resonances. We note that the lifetimes of the members of the doublet at 4.92 and 4.94 MeV differ by a factor of at least 12.

C. J^π Assignments

The lifetime data presented above provide additional information on J^π assignments for three bound states. Each case is considered separately as follows.

2.722-MeV Level

The angular-correlation and linear-polarization measurements discussed in previous sections resulted in the possibilities $J^\pi(2.72)=1^-$, 2^+, or 2^-. The lifetime $\tau_m(2.72)=0.96\times10^{-13}$ sec and the possible mixing ratios (Table VI) for the 2.72→0 transition lead to the unreasonably high $M2$ strengths $|M|^2(M2)\geq50$ and 120, respectively, for the 1^- and 2^- cases. On the other hand, for $J^\pi(2.72)=2^+$, the reasonable values $|M|^2(M1)=0.0016$ and $|M|^2(E2)=9.2$ result.

4.425-MeV Level

This level was shown to have $J=2$ by the angular-correlation data at the 1749-keV resonance. The same data also show that the 4.43→0 transition is nearly pure quadrupole ($\delta=-19_{-10}^{+5}$). This result, when combined with the observed lifetime $\tau(4.43)=(6.4\pm0.8)\times10^{-14}$ sec shows that the 4.43-MeV level has even parity. For odd parity, an $M2$ strength of at least 40 Weisskopf units is implied, while for even parity the $E2$ strength is 1.3 Weisskopf units.

4.921-MeV Level

The angular-correlation and polarization data show that this level is either 3^- or 5^-. Its dominant decay (90%) to the 4.23-MeV level (4^-), the only other transition being a weak (10%) branch to the 1.45-MeV level (2^+), suggests that the correct assignment is 5^-. Support for the 5^- assignment is given by considerations of the transition speeds. For $J^\pi(4.92)=3^-$, and the experimental lower limit $\tau(4.92)\geq8\times10^{-13}$ sec, we have the following results:

Transition	δ	$\lvert M\rvert^2(E1)$	$\lvert M\rvert^2(M1)$	$\lvert M\rvert^2(E2)$	$\lvert M\rvert^2(M2)$
4.92→1.45	−0.73	$\leq2.0\times10^{-6}$			≤0.40
4.92→4.23	+0.29		$\leq8.5\times10^{-2}$	≤80	

The upper limit of the $E1$ transition speed is 100 times slower than the average for $\Delta T=0$ $E1$ transitions in $20\leq A\leq40$ nuclei.[34] Furthermore, if we make the conservative assumption that the *actual* lifetime is such that the $E2$ strength is ≤15 Weisskopf units (10 times the average $\Delta T=0$ $E2$ strength), then the $E1$ speed is $\leq4\times10^{-7}$ Weisskopf units. Also, the possible but unobserved $E1$ transitions to the 1.97-, 2.54-, and 2.72-MeV levels would each have a strength less than about 10^{-7} Weisskopf units.

Similar considerations for $J^\pi(4.92)=5^-$ lead to more reasonable results. If we assume the lifetime is such that the 4.92→1.45, $E3$ strength is less than 15 Weisskopf units (the average[34] is 6.3 with a "70%" spread factor of 2.2), then the following results are obtained.

Transition	δ	$\lvert M\rvert^2(M1)$	$\lvert M\rvert^2(E2)$	$\lvert M\rvert^2(E3)$
4.92→1.45	0			≤15
4.92→4.23	−0.29	$\leq1.9\times10^{-3}$	≤1.8	

The $M1$ and $E2$ speeds so implied are very close to the averages of 1.8×10^{-3} and 0.8 obtained in the present work (Sec. IX) for other $\Delta T=0$ transitions in P^{30} and to those for $20\leq A\leq40$ nuclei obtained by Skorka *et al.*[34]

The 4.92-MeV level is thus very probably 5^-. A 3^- assignment is not regarded as entirely excluded, although it would appear difficult to explain in this case the inhibition of the several possible $E1$ transitions by at least a factor of 10^3 over the usual inhibition of 10^4 for $\Delta T=0$ $E1$ transitions.

VIII. SUMMARY AND SYNTHESIS OF DATA

A. Resonance Level Properties

The proton energies, corresponding excitation energies in P^{30}, strengths, and total widths of the 24 observed

TABLE XI. Properties of resonance levels of P^{30}. The quantities ϵ and x are the amplitude ratios of capture by orbital momenta $(l+2)/l$ and by total proton momenta j_p'/j_p in jj coupling, respectively. The T assignments result from considerations of the decay-scheme properties. $I(T=1)$ is the total fractional "reduced" branching to $T=1$ levels (see text).

E_p (keV)	J^π	T	$I(T=1)$ (%)	$P(0)$	ϵ	x^2	θ_p^2 (10²)	Comments
327	$1, 2^-$		0					a, b
416	1	(0)	73	0.56 ± 0.02				c, d
698	2^-		0	0.42 ± 0.06	$-1.6\leq\epsilon\leq0.44$		≥0.064	c, e
731	3^+	0	98	0.47 ± 0.13	$\lvert\epsilon\rvert\geq0.73$		≥0.22	c, f, e
917	1	0	97	0.32 ± 0.05				c
958		0	82					
1111		0	97					
1302	1	0	97	0.33 ± 0.03				c
1324	3, (2)	(0)	64					a
1327	2^-		7	0.41 ± 0.03	$\lvert\epsilon\rvert\leq0.19$		29	a, f, e, g
1374	1^-	0	92	0.94 ± 0.03		1.9 or 10	32	c, h
1470	2^-	0	56	0.44 ± 0.04	-0.16 ± 0.16 or 1.6 ± 0.5		$\simeq2$	c, e, h
1502								
1505	4^-	1	0	0.44			13	e, i, j
1643	1^-	(1)	9	0.51 ± 0.02		0.21 or 23	28	k
1664		0	98					
1669			0					
1686	2^-	1	0	0.43 ± 0.12	$\lvert\epsilon\rvert\leq0.45$		8.2	f, e, k
1746	3	0	80	0.33 ± 0.07				c
1749	2^+	(1)	1	0.24 ± 0.09		$0.12\leq x^2\leq1.3$	≥0.006	l
1773		0	90					
1775	3, (1)	(0)	67					a
1792	1^-	0	~90				21	m

[a] Two J values consistent with angular-correlation data.

[b] See Table IV for $P(0)$. $\theta_p^2(l=2)=2.5$ if $J^\pi=2^+$. For 2^-, $P(0)=0.40\pm0.04$, $\theta_p^2(l=1)\geq0.15$, and $\lvert\epsilon\rvert\leq0.10$.

[c] Spin (and parity) determined uniquely by angular-correlation (and polarization) data.

[d] If $J^\pi=1^+$, $P(0)$ and resonance strength imply $\theta_p^2(l=2)\geq0.16$.

[e] Value of θ_p^2 given corresponds to the lower-order orbital momenta which can contribute.

[f] Value of $P(0)$ and limit of ϵ chosen such that the Wigner limit is not exceeded by the higher-order angular momenta which may contribute to the capture.

[g] Resonance clearly corresponds to $J^\pi=2^-$ resonance in (p, p) data (see Table I).

[h] Observed as $l=1$ resonance in (p, p) data (Ref. 22). The width of the 1470-keV resonance, as determined in a preliminary analysis of our recent (p, p) data, is approximately $\Gamma_p=0.7$ keV, thus $\theta_p^2\simeq0.02$.

[i] $P(0)=0.44$ corresponds to assumed pure f-wave capture.

[j] Split, 4^- analog state with members separated by 700 eV. θ_p^2 for the separate members, determined by (p, p) measurements, are given in the Appendix.

[k] J determined uniquely by angular correlations. Parity determined by correspondence with (p, p) data (Table I).

[l] J determined uniquely by angular correlations. $J^\pi=2^-$ would imply $\lvert M\rvert^2(M2)=11$ for the $R\to0.68$ transition.

[m] J^π and resonance width from Ref. 22.

resonances are given in Table I. The resonance decay schemes are given in Table II, and revised decay schemes for several bound levels in Table III. Spins and parities for many of the resonances have been derived from the angular-correlation and polarization data (Secs. V and VI). In a few other cases, the spin and/or parity can be deduced from additional considerations based on transition speeds or by comparison with the elastic-scattering data.[22] The results are given in Table XI. This Table also lists the values of $P(0)$, the corresponding ratios x^2 in some cases of j_p' to j_p formation from Eq. (4) or the ratios ϵ of formation by proton orbital momenta $l+2$ and l from Eq. (3), the reduced proton widths, and isobaric spin. The reduced widths are based upon a radius $R=1.2(A^{1/3}+1)$ F. The isobaric spin (or more precisely, the dominant T component) is assigned in cases where the effect of the $\Delta T=\pm1$ selection rule clearly prevails, or as in the cases of the 1505- and 1686-keV resonances, where the decay scheme is clearly dominated by "analog-to-antianalog" type transitions.[38]

Resonance assignments of $T=0$ can be made in many cases with considerable confidence by consideration of the values of the total fractional "reduced branching" $I(T=1)$ to $T=1$ levels given in Table XI. These values were derived from the decay-scheme data in Table II for each resonance by removing the energy dependence (E_γ^3 for dipole radiation) from each transition and reconstructing a decay scheme of "reduced branching ratios." One finds in many of the decay schemes so constructed that the total fractional branching to the relatively small subset of $T=1$ levels is much

[38] See Ref. 6 or, for example, P. M. Endt, Aerospace Research Laboratories Report No. ARL 66-0221 (unpublished) for more detailed discussion of "analog-to-antianalog" transitions in s-d shell nuclei.

TABLE XII. Multipolarity mixing ratios of transitions from resonance levels in P^{30}.

Resonance E_p (keV)	Final state (MeV)	$J_i^\pi \rightarrow J_f^\pi$	δ
416	0	$1\rightarrow 1^+$	-0.02 ± 0.10 or $\lvert\delta\rvert \geq 8.1$
	0.71	1^+	-0.02 ± 0.04
698	0	$2^-\rightarrow 1^+$	-0.18 ± 0.08 or $5.2_{-1.2}^{+3.0}$
	0.71	1^+	-0.11 ± 0.05
	1.97	3^+	0.05 ± 0.03
	2.54	3^+	0.08 ± 0.08
	2.72	2^+	-0.04 ± 0.04
731	2.94	$3^+\rightarrow 2^+$	-0.02 ± 0.02
	4.18	2^+	-0.04 ± 0.02
917[a]	4.50	$1\rightarrow 1^+$	0.22 ± 0.23 or $-4.5_{-\infty}^{+2.4}$
1302[a]	2.94	$1\rightarrow 2^+$	0.22 ± 0.16
1322	1.97	$3^+\rightarrow 3^+$	0.14 ± 0.20 or $-1.4_{-0.8}^{+0.5}$
	2.94	2^+	-0.03 ± 0.05
1327	0	$2^-\rightarrow 1^+$	0.03 ± 0.06
1374	1.45	$1^-\rightarrow 2^+$	-0.05 ± 0.03
1470	0	$2^-\rightarrow 1^+$	0.03 ± 0.02
	0.71	1^+	0.02 ± 0.02
	3.02	1^+	-0.06 ± 0.05
	4.14	2^-	0.02 ± 0.04
	4.50	1^+	-0.04 ± 0.03
1505	1.97	$4^-\rightarrow 3^+$	0.02 ± 0.02
	2.54	3^+	-0.08 ± 0.03
	2.84	3^+	-0.02 ± 0.03
	4.23	4^-	0.00 ± 0.02
	4.62	3^-	-0.07 ± 0.03
	4.92	$(5)^-$	(0.05 ± 0.03)
1643	0	$1^-\rightarrow 1^+$	0.00 ± 0.05
	3.02	1^+	0.04 ± 0.03
1686	0	$2^-\rightarrow 1^+$	0.03 ± 0.02
	0.71	1^+	0.02 ± 0.03
	1.45	2^+	0.07 ± 0.05
	4.14	2^-	-0.02 ± 0.01
1746	1.45	$3\rightarrow 2^+$	-0.05 ± 0.02
	2.94	2^+	0.02 ± 0.03
1749	0	$2^+\rightarrow 1^+$	-0.05 ± 0.04 or 3.5 ± 0.5
	2.72	2^+	0.17 ± 0.07
	4.43	2^+	-0.01 ± 0.03
	4.94	$1^{(+)}$	-0.21 ± 0.05
1775	2.94	$(3)\rightarrow 2^+$	(-0.23 ± 0.05)

[a] Mixing ratios obtained from triple correlations not discussed in text.

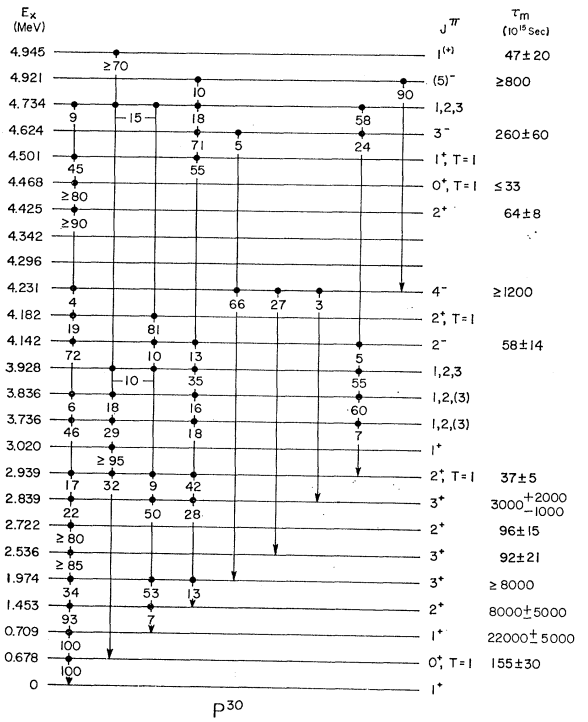

FIG. 22. Summary of bound levels in P^{30}. The properties of the 3.73-, 3.84, and 3.93-MeV levels, and the decay of the 2.84-MeV level, are from Ref. 9. The lifetime of the 0.68-MeV level is from Ref. 10, and the lifetimes of the 0.71-, 1.45-, 1.97-, and 2.84-MeV levels are taken from Ref. 40. The remaining information, except the J^π, T values for P^{30} (0) and P^{30} (0.68), results from the present work and Paper I.

higher than would be expected if there were no effect due to isobaric-spin selection rules. If, for example, the decay schemes were governed only by a spin selection rule $\Delta J=0, \pm1$; the expected values of $I(T=1)$ would be approximately 28, 8, and 2% for $J_R=1$, 2, and 3, respectively. However, for 10 of the observed resonances, the value of $I(T=1)$ is greater than 80%. In these cases $T=0$ is assigned because of the clear effect of the $\Delta T=\pm1$ selection rule. For 3 other resonances $I(T=1)$ is greater than 64%, so a probable $T=1$ assignment is made. A small value of $I(T=1)$, on the other hand, is not, by itself, a good indication of $T=1$ for a resonance because of the small values expected for random decay governed by ordinary spin selection. Additional support for the T assignments is gained from consideration of average $E1$ transition speeds and a more detailed analysis of isobaric-spin mixing (Sec. IX).

B. Multipolarity Mixing Ratios

The mixing ratios δ obtained from the angular-correlation data for transitions from the resonance levels are collected in Table XII. In a few cases, a second solution from the angular-correlation data has been eliminated by consideration of the corresponding transition speeds derived from the resonance strengths. At the 1749-keV resonance, the strength $S=5.2$ eV (Table I) and the

TABLE XIII. Multipolarity mixing ratios of transitions between bound states of P^{30}. $\langle\delta\rangle$ represents the weighted average of δ values obtained at two or more resonances.

Initial state (MeV)	Final state (MeV)	$J_i^\pi \to J_f^\pi$	Source resonance (keV)	δ	$\langle\delta\rangle$
0.71	0	$1^+ \to 1^+$	416	-0.25 ± 0.05 or $-4.2_{-1.1}^{+0.7}$	-0.22 ± 0.02 or $-4.5_{-0.5}^{+0.3}$
			1470	-0.27 ± 0.04 or $-3.7_{-0.6}^{+0.5}$	
			1505	-0.16 ± 0.06 or $-6.3_{-4.0}^{+1.7}$	
			1686	-0.19 ± 0.03 or $-4.7_{-0.7}^{+0.6}$	
1.45	0	$2^+ \to 1^+$	731	0.29 ± 0.07	0.22 ± 0.02
			1374	0.25 ± 0.03	
			1470	0.20 ± 0.04	
			1505	0.21 ± 0.03	
			1746	0.15 ± 0.04	
1.97	0	$3^+ \to 1^+$	1505	0.02 ± 0.03	
	0.71	$3^+ \to 1^+$	1505	-0.01 ± 0.02	
2.54	0	$3^+ \to 1^+$	1505	0.02 ± 0.03	
2.72	0	$2^+ \to 1^+$	698	$-3.3_{-0.6}^{+0.8}$	-3.0 ± 0.4 [a]
			1746	$-2.7_{-0.8}^{+1.0}$	
2.94	0	$2^+ \to 1^+$	731	0.08 ± 0.04 or 1.9 ± 0.3	
	1.45	$2^+ \to 2^+$	731	0.03 ± 0.03	
4.14	0	$2^- \to 1^+$	1686	0.01 ± 0.01	
4.18	0.71	$2^+ \to 1^+$	731	-0.01 ± 0.08 or $2.9_{-0.5}^{+0.8}$	
4.23	1.97	$4^- \to 3^+$	1505	-0.05 ± 0.02	
	2.54	$4^- \to 3^+$	1505	0.00 ± 0.02	
4.43	0	$2^+ \to 1^+$	1749	-19_{-10}^{+5}	
4.50	0	$1^+ \to 1^+$	1470	0.09 ± 0.04 or $9.5_{-2.8}^{+7.0}$	
	1.45	$1^+ \to 2^+$	1470	-0.01 ± 0.03	
4.62	1.45	$3^- \to 2^+$	1505	-0.01 ± 0.02	
4.92	1.45	$(5)^- \to 2^+$	1505	0 [b]	
	4.23	$(5)^- \to 4^-$	1505	-0.29 ± 0.04	

[a] A value $\delta = -0.82\pm0.07$ has been eliminated by combining the results of polarization and lifetime measurements with the angular-correlation results.

[b] Transition assumed to be pure octupole.

nonzero value of the mixing ratio $\delta(R \to 4.94)$ lead to a tentative even-parity assignment for the 4.94-MeV level.

In Table XIII are given the multipolarity mixings for transitions between bound states of P^{30}. In cases where a given mixing ratio was measured at two or more resonances, the weighted average value is computed. In such cases, the agreement between values from different resonances is seen to be good except for the 1.45→0 transition at the 1746-keV resonance. It was given low weight in the average for reasons discussed in Sec. V C. It is interesting that each of the 2^+ levels at 1.45, 2.72, and 4.43 MeV decay to the ground state by highly mixed $M1$-$E2$ radiation. It can be shown that the mixing-ratio ambiguities in the ground-state transitions from the 1^+ levels at 0.71 and 4.50 MeV are impossible to eliminate by angular-correlation and linear-polarization measurements.

C. Transition Strengths

The strengths, in Weisskopf units,[39] of transitions between low-lying levels in P^{30}, computed from the lifetime, decay-scheme, and multipolarity-mixing data already presented, are given in Table XIV. The strengths are given for $\delta=0$ unless the measured value differs from zero by at least two times the quoted error. In a few specifically noted cases, the assumption $\delta=0$ is used although the actual value is not known.

The strengths of transitions from the 0.71-, 1.45-, 1.97-, and 2.84-MeV levels are based upon the mean lifetimes 0.71 (22±5 psec), 1.45 (8±5 psec), 1.97 (>8 psec), and 2.84 ($3_{-1.0}^{+2.0}$ psec) reported recently by Pixley and Poletti.[40] The result given for the 2.84-MeV level yields even parity by considerations similar to those discussed in Sec. VII C.

D. Summary of Bound-State Properties

The information presented schematically in Fig. 22, taken with the multipolarity-mixing data and derived transition strengths given in Tables XIII and XIV, summarizes most of the presently available information on levels below 5 MeV in P^{30}. The decay schemes for the 2.839-, 3.736-, 3.836-, 3.928-, and 4.734-MeV levels, and

[39] D. H. Wilkinson in *Nuclear Spectroscopy*, edited by Fay Ajzenberg-Selove (Academic Press Inc., New York, 1960), Part B.

[40] R. E. Pixley and A. R. Poletti, Bull. Am. Phys. Soc. **14**, 125 (1969).

TABLE XIV. Strengths in Weisskopf units of transitions in P^{30}.

E_i (MeV)	E_f (MeV)	$J_i^\pi \to J_f^\pi$	$T_i \to T_f$	δ[a]	$\lvert M\rvert^2(E1)$ (10^4)	$\lvert M\rvert^2(M1)$ (10^2)	$\lvert M\rvert^2(E2)$	$\lvert M\rvert^2(M2)$	$\lvert M\rvert^2(E3)$
0.68[b]	0	$0^+ \to 1^+$	$1 \to 0$	0		65			
0.71[c]	0	$1^+ \to 1^+$	$0 \to 0$	−0.22		0.32	1.8		
				−4.5		0.018	2.9		
1.45[c]	0	$2^+ \to 1^+$	$0 \to 0$	0.22		0.093	0.10		
	0.71	$2^+ \to 1^+$	$0 \to 0$	b		0.057			
1.97[c]	0	$3^+ \to 1^+$	$0 \to 0$	0			≤ 0.18		
	0.71	$3^+ \to 1^+$	$0 \to 0$	0			≤ 2.5		
	1.45	$3^+ \to 2^+$	$0 \to 0$			≤ 0.31			
2.54	0	$3^+ \to 1^+$	$0 \to 0$	0			15		
2.72	0	$2^+ \to 1^+$	$0 \to 0$	−3.0		0.16	9.2		
2.84[c]	0	$3^+ \to 1^+$	$0 \to 0$	b			0.048		
	0.71	$3^+ \to 1^+$	$0 \to 0$	b			0.46		
	1.45	$3^+ \to 2^+$	$0 \to 0$	b		0.092			
2.94	0	$2^+ \to 1^+$	$1 \to 0$	0.08		0.56	0.019		
				1.9		0.12	2.4		
	0.68	$2^+ \to 0^+$	$1 \to 1$	0			21		
	0.71	$2^+ \to 1^+$	$1 \to 0$			0.68			
	1.45	$2^+ \to 2^+$	$1 \to 0$	0		11			
4.14	0	$2^- \to 1^+$	$0 \to 0$	0	1.7				
	0.71	$2^- \to 1^+$	$0 \to 0$		0.43				
	1.45	$2^- \to 2^+$	$0 \to 0$		1.2				
	2.94	$2^- \to 2^+$	$0 \to 1$		5.1				
4.23	0	$4^- \to 1^+$	$0 \to 0$						≤ 40
	1.97	$4^- \to 3^+$	$0 \to 0$	−0.05	≤ 0.46			≤ 0.11	
	2.54	$4^- \to 3^+$	$0 \to 0$	0	≤ 0.48				
4.43	0	$2^+ \to 1^+$	$0 \to 0$	−19		0.0015	1.3		
4.47	0	$0^+ \to 1^+$	$1 \to 0$	0		≥ 1.1			
4.62	1.45	$3^- \to 2^+$	$0 \to 0$	0	0.86				
	1.97	$3^- \to 3^+$	$0 \to 0$		0.11				
	2.94	$3^- \to 2^+$	$0 \to 1$		2.0				
4.92	1.45	$(5)^- \to 2^+$	$0 \to 0$	0					≤ 670
	4.23	$(5)^- \to 4^-$	$0 \to 0$	−0.29		≤ 8.5	≤ 80		

[a] Where no value is given, δ is assumed to be zero.
[b] Transition strengths based upon lifetime given in Ref. 10.
[c] Transition strengths based upon lifetimes given in Ref. 40.

their possible spins except for the 2.839-MeV level, are taken from Vermette *et al.*[9] However, we have enclosed their possible $J=3$ assignments for the 3.736- and 3.836-MeV levels in parentheses to indicate the improbability of levels with $J>2$ and the observed decay properties. The lifetime of the level at 0.678 MeV is from Ref. 10, and those for the 0.71-, 1.45-, and 2.84-MeV levels are from Ref. 40. The J^π, T assignments for the ground state and 0.678-MeV level are from Ref. 7 (see Introduction). (All levels are $T=0$ except those denoted $T=1$.) The remaining information is from the present work and Paper I.

IX. DISCUSSION

Much new spectroscopic information on levels of P^{30} has been obtained with a variety of techniques involving the proton-capture reaction. Most of the previously reported results have been reexamined and improved or verified. The results demonstrate, we believe, the high yield of information obtainable from the capture reaction, especially with the use of the large-volume Ge(Li) detectors. It is also clear, of course, that the availability of information from other reactions [in this case from (d, α),[15] (p, p) [22,23] and $(He^3, p\gamma)$ [9]] is of great value for supplementing and interpreting the capture data. In the following paragraphs, some special aspects and implications of the data are discussed.

A. Transition Rates, Isospin Impurity, and Coulomb Interaction

The availability of the strengths of over 50 transitions in P^{30} between levels of assigned J^π and T makes possible an extraction of average isospin impurities, and an estimate of the average Coulomb perturbation energy. In Table XV, we show the average transition strengths in P^{30} and compare them with those obtained by Skorka *et al.*[34] for $20 \leq A \leq 40$. The averages and 70% width factors were computed in the manner used by Skorka *et al.* The number of examples available in P^{30} is about 30% of that considered for the entire range $20 \leq A \leq 40$.

TABLE XV. Average transition strengths $\langle|M|^2\rangle$ in P^{30} compared with those compiled by Skorka *et al.* (Ref. 34) for nuclei with $20\leq A\leq 40$.

Transition type	P^{30} Examples	$\langle|M|^2\rangle$	70% Width	$20\leq A\leq 40$ Examples	$\langle|M|^2\rangle$	70% Width
$E1(\Delta T=0)$	11	$1.6(10^{-4})$	4.3	19	$1.8(10^{-4})$	7.2
$E1(\Delta T=1)$	13	$2.2(10^{-3})$	4.3	60	$1.5(10^{-3})$	6.6
$M1(\Delta T=0)$	10	$1.8(10^{-3})$	7.8	12	$8.8(10^{-3})$	3.4
$M1(\Delta T=1)$	18	0.11	5.9	16	0.20	7.2
$E2(\Delta T=0)$	9	0.79	13.2	87	1.5	10.0
$E2(\Delta T=1)$	5	0.51	2.6	3	0.44	12.0
$M2(\Delta T=1)$	3	0.10	3.1	11	0.087	5.0

There is close agreement between the average strengths. The greatest difference is in the $\Delta T=0$, $M1$ transitions, which are about a factor of 5 lower in P^{30}.

The $\Delta T=1$, $E2$ transitions are on the average somewhat slower than $\Delta T=0$, $E2$ transitions. This result is expected since no collective enhancement of $\Delta T=1$, $E2$ transitions in self-conjugate nuclei is possible in the weak-coupling approximation.[41] Specific examples of collective enhancement of $\Delta T=0$, $E2$ transitions appear to be the 2.94→0.68, 2.54→0, and 2.72→0 transitions with $|M|^2=21$, 15, and 9.2, respectively (Table XIV). The average $M2$ speed agrees almost exactly with that found by Skorka *et al.*

Figure 23 compares the histograms of T-allowed and T-forbidden $E1$ and $M1$ transitions in P^{30} with those for $20\leq A\leq 40$. (This figure and Table XV includes transitions from resonance levels.) There appears to be a somewhat more marked separation between the T-forbidden and -allowed transitions in P^{30} than in the samples for $20\leq A\leq 40$. This observation is consistent, except for the $\Delta T=0$, $M1$ transitions, with the smaller 70% widths for P^{30} shown in Table XV. A larger spread of the $20\leq A\leq 40$ results could be expected as an effect due to the authenticated mass dependence of the transition strengths.[34] The large spread in the $\Delta T=0$, $M1$ strengths in P^{30} perhaps reflects both the possibility of near cancellation due to the relative phases of various parts of the $M1$ matrix element,[41,42] and the l-forbiddeness of $s\rightarrow d$ single-particle transitions. Such effects may, for example, explain the very low strength, $|M|^2=1.5\times10^{-5}$, of the $M1$ part of the 4.43→0 (2^+, 0→1^+, 0), transition and the consequent high value, $\delta=19$, for the $M1$-$E2$ mixing ratio. On the average, $\Delta T=0$, $M1$ strengths in P^{30} are weaker than the $\Delta T=1$, $M1$ strengths by a factor of 60, in reasonable agreement with the factor of 100 stated in the $M1$ selection rule by Morpurgo.[43] The value for P^{30} is considerably higher, however, than the retardation factors of 5 and 10 reported recently by Lawergren[44] for Mg^{24} and Si^{28}, respectively.

Following Lawergren[44] and Warburton,[41] we express the ratio R of reduced rates of $M1$ transitions with $\Delta T=0$ and $\Delta T=1$, respectively, by

$$R=[-(1.8+\langle G_0\rangle)/(9.4+\langle G_1\rangle)]^2,$$

where $G_{\Delta T}$ contains the angular and spin dependence of the $M1$ matrix element. Using the assumption $\langle G_0\rangle=\langle G_1\rangle$, we find $\langle G\rangle=-2.7$ for P^{30}. The values for Mg^{24} and Si^{28} found by Lawergren are -3.8 and -3.7, respectively. The value for P^{30} is closer to the theoretical estimate $\langle G\rangle=-2$ obtained by Lawergren for transitions between $1d_{5/2}$, $1d_{3/2}$, and $2s_{1/2}$ states.

The average T admixture in the wave functions can be estimated from the set of $E1$ transition strengths. The amplitude $\alpha_T(T')$ of the admixture of states with

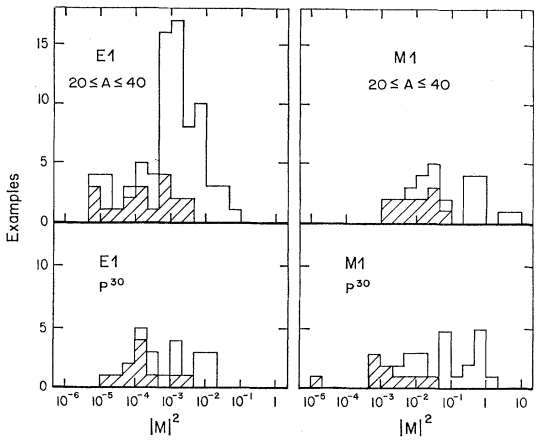

FIG. 23. Histograms of $E1$ and $M1$ transition strengths, in Weisskopf units, in P^{30} compared with those compiled by Skorka *et al.* (Ref. 34) for $20\leq A\leq 40$. The T-forbidden transitions are indicated by the cross-hatching.

[41] E. K. Warburton, in *Isobaric Spin in Nuclear Physics*, edited by J. D. Fox and D. Robson (Academic Press Inc., New York, 1966).

[42] J. B. Marion, in *Nuclear Research with Low Energy Accelerators*, edited by J. B. Marion and D. M. Van Patter (Academic Press Inc., New York, 1967).

[43] G. Morpurgo, Phys. Rev. **110**, 721 (1958).

[44] B. T. Lawergren, Nucl. Phys. A111, 652 (1968).

$\psi(T')$ in states ψ, where

$$\psi=\psi(T)+\sum_{T'}\alpha_T(T')\psi(T')$$

is given by

$$\alpha_T{}^2(T')=\frac{\langle|M|^2E1\rangle(\Delta T=0)}{\langle|M|^2E1\rangle(\Delta T=1)}.$$

We obtain for levels below 7 MeV in P^{30}, $\alpha_T{}^2(T')=0.073$, a value somewhat smaller than the average of 0.12 for $20\leq A\leq 40$ nuclei,[34] and the values 0.5 and 0.15 for Mg^{24} and Si^{28}.[44] However, the radiating levels considered in Mg^{24} and Si^{28} are typically at $\approx$12-MeV excitation where one expects a greater level density and consequently a greater isospin mixing.

The T admixture may be considered to arise from the Coulomb perturbation $H_{TT'}{}^C$ between levels with isospin T and T' with energy separation $\Delta_{TT'}$. In first-order perturbation theory, $\alpha_T(T')=H_{TT'}{}^C/\Delta_{TT'}$. The average separation $\langle\Delta_{TT'}\rangle=180$ keV for levels in P^{30} in the region $E_x=5.9$–7.5 MeV with the same J^π is estimated from the level schemes of Si^{30} and P^{30}. The resultant average value for the Coulomb perturbation is then $\langle H_{TT'}{}^C\rangle=50$ keV, to be compared with the values 30 and 15 keV for Mg^{24} and Si^{28}, respectively.[44]

B. T-Mixed Doublet in P^{30}

As emphasized recently by Marion,[42] it is virtually impossible to determine precisely the amount of T mixing in a single level without reference to the associated level (or levels) with which the mixing occurs. If, however, the two members A and B of a T-mixed doublet can be identified, where in a T representation

$$|A\rangle=\alpha|T=0\rangle+\beta|T=1\rangle$$

and

$$|B\rangle=\beta|T=0\rangle-\alpha|T=1\rangle$$

the coefficients α and β may be determined by use of the strong $E1$ selection rule for decay of the two levels to a lower final state with opposite parity and (hopefully) well-defined T. For a final state (e.g., the ground state) with $T=0$, the ratio $|M(E1)|_A{}^2/|M(E1)|_B{}^2=\beta^2/\alpha^2$.

Examination of the properties of the 1^- and 2^- resonance levels in P^{30} shows behavior in some cases suggestive of T mixing between pairs. A clearly identifiable case is represented by the 2^- resonances at $E_p=$ 1470 and 1686 keV. The properties of these resonances are compared in Fig. 24. The strength, width, and decay-scheme properties of the 1686-keV resonance suggest that it is the main component of a $T=1$ analog state. It exhibits a strong $2^-\rightarrow 2^-$, $M1$ transition typical of many other observed analog-to-antianalog decays. $E1$ transitions to $T=0$ levels only are observed. The 1470-keV resonance has an almost identical, but weaker, $E1$ decay scheme to the same $T=0$ levels. Significantly, however, it has a strong $E1$ transition to the 1^+, $T=1$

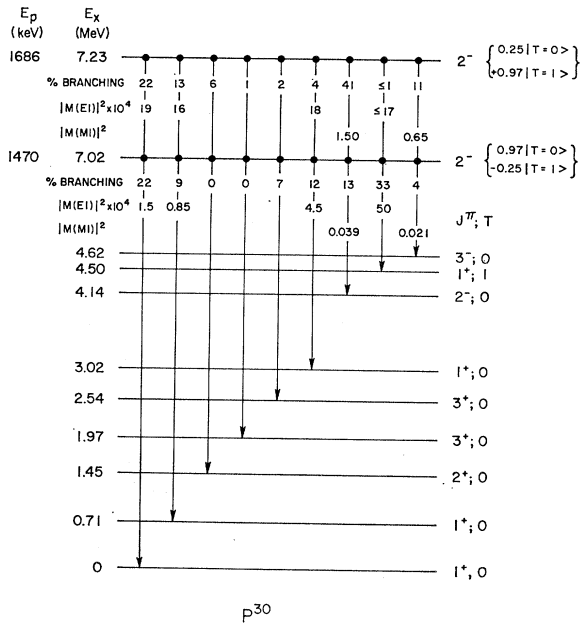

FIG. 24. Schematic comparison of the γ-ray decay properties of the 2^- resonances at $E_p=1470$ and 1686 keV. The relative intensities of transitions from each resonance are indicated along with the absolute intensities in Weisskopf units. The detailed comparison shows that these two resonances are members of a T-admixed pair as discussed in the text. The deduced wave functions in a T representation are shown.

level at 4.50 MeV which is not observed at the 1686-keV resonance. For our present purpose, the ground state and 0.71-MeV level can be regarded as pure $T=0$. Also, since the branching ratios for decay to these two levels are better determined than those to higher levels, we use these transitions to find the ratio β^2/α^2 in the case where $|A\rangle=|1470\rangle$ and $|B\rangle=|1686\rangle$. We find $\beta^2/\alpha^2=0.067$ and thus $\alpha=0.97$ and $\beta=0.25$. The value of $H_{TT'}{}^C$ corresponding to this result and the level separation $\Delta_{TT'}=216$ keV is 56 keV, a value very close to the rough average value of 50 keV obtained above. We see that the relative $M1$ transitions from the two resonances behave as expected if it is assumed that the $M1$ transitions, like the $E1$ transitions, are hindered for $\Delta T=0$. Also the $R(2^-)\rightarrow 4.14(2^-)$ analog-to-anti-analog transition appears at both resonances; but weaker, as expected, at the 1470-keV resonance which has the smaller $T=1$ component.

C. Odd-Parity Levels in P^{30}

An interesting feature of P^{30} is the presence of several strong odd-parity resonances near $E_x=7$ MeV with large proton reduced widths, and the strong decay of some of them to members of the set of four $T=0$ levels with $J^\pi=2^-$, 3^-, 4^-, and $(5)^-$ in the region $E_x=4$–5 MeV. The three 1^- resonances at $E_p=1374$, 1643, and 1792 keV have a total reduced width of $\theta_p{}^2=0.81$ for p-wave proton capture (Table XI). The relative contribution of $p_{1/2}$ and $p_{3/2}$ capture cannot be determined

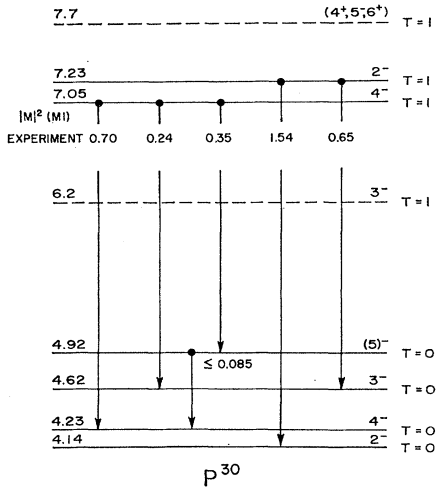

FIG. 25. Spectrum of odd-parity levels in P^{30}. The levels indicated at $E_x=6.2$, and 7.7 MeV are deduced from the positions of known levels in Si^{30}. The observed $M1$ transition strengths are shown.

uniquely from the present data. However, the two possible values for the ratio $x^2=p_{3/2}/p_{1/2}$ are given in Table XI for the 1374- and 1643-keV resonances. Clearly, isobaric spin would also have to be considered in any detailed analysis of the reduced widths because, as indicated in the Table, the 1643-keV resonance is probably mostly $T=1$, whereas the other two are mainly $T=0$. Although a detailed analysis is not presently possible, it is clear that these three 1^- resonances must account for a significant fraction of the $2p_{3/2}$ (and/or $2p_{1/2}$) strength in P^{30}. A similar observation can be made about the 2^- resonances at $E_p=1327$, 1470, and 1686 keV. The dominant mode of formation is by $p_{3/2}$ capture with a total reduced width $\theta_p^2=0.4$. Finally, a strength $\theta_p^2=0.13$ for $f_{7/2}$ capture is found at $E_p=1505$ keV.

The spectrum of $T=0$ odd-parity states between 4 and 5 MeV and the $T=1$ resonances ($E_p=1505$ and 1686 keV) which decay strongly to these by $M1$ transitions is shown in Fig. 25. The $T=1$ levels indicated by dashed lines have not been observed in P^{30}, but are expected as analogs of known levels in Si^{30}. The possibility has been considered[45] that this experimental spectrum corresponds to a relatively pure $(d_{3/2}$-$f_{7/2})$ two-nucleon spectrum. In this spectrum, one expects a set of levels with $T=0$ and a set with $T=1$ with their $(2J+1$ weighted) centers of gravity separated by about 3 MeV due to the $\mathbf{T}_0\cdot\mathbf{t}$ interaction.[46] Each set should have four members with $J^\pi=2^-$, 3^-, 4^-, and 5^-. The center-of-gravity separation of the experimental spectra shown is 2.6 MeV. The corresponding value of the parameter V_1 in the isospin monopole-interaction term $(V_1/A)\mathbf{T}_0\cdot\mathbf{t}$ is 78 MeV which compares with the values $V_1=102$ and 105 MeV obtained from $1f_{7/2}$ analog and antianalog states in Cl^{35} and Cl^{37}, respectively.[47] Also, the 2^-, $T=0$ state lies lowest in the spectrum in accordance with the first Nordheim rule[48] for a particle-particle (or hole-hole) configuration consisting of $d_{3/2}$ and $f_{7/2}$ orbitals.

This odd-parity spectrum can be compared with the results obtained by Kim Dong-Hyok[49] using the $Si^{28}(\alpha, d)P^{30}$ reaction with $E_\alpha=29$ MeV. At this energy, the average angular momentum transferred by the two nucleons is about 4 to $5\hbar$ at small angles. Most of the strong levels observed in this reaction were then identified as probable $(d_{3/2}f_{7/2})$ states. The published deuteron energy spectrum at a laboratory angle of 30° shows relatively weak peaks corresponding to the even-parity levels below $E_x=3$ MeV in P^{30}. Above 3 MeV, however, strong peaks are present at $E_x=4.17$, 4.90, 5.70, 7.11, 8.0, and 9.25 MeV, with uncertainties in energy, where given, between ±50 and ±100 keV. The dominant peaks in the spectrum are those at $E_x=$ 4.17 and 7.11 MeV. Thus there is a close correspondence between the deuteron spectrum and the odd-parity spectrum shown in Fig. 25.

These general observations, however, provide little insight into the likely influence of strong admixtures of configurations such as $(s_{1/2}f_{7/2})$ in the 3^- and 4^- levels,

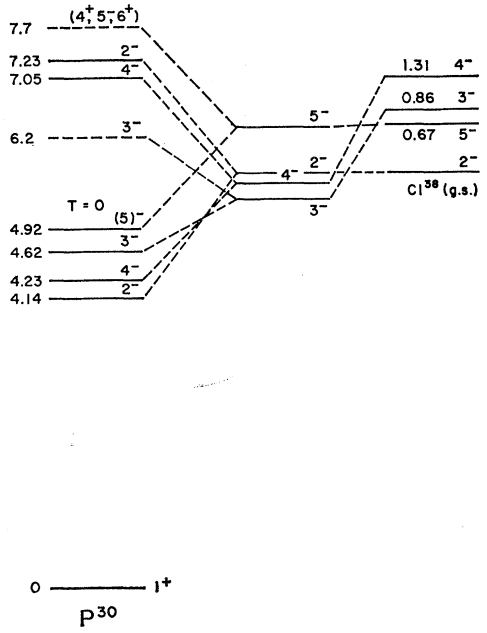

FIG. 26. Comparison of the two-nucleon spectrum of P^{30} with the known $(d_{3/2}f_{7/2})$ two-particle spectrum of Cl^{38}. Except for a J-independent constant, the energy-averaged spectrum (center) should be comparable to the Cl^{38} spectrum as discussed in the text. Note the close correspondence between the 2^- and 5^- levels but the rather large relative displacement of the 3^- and 4^- levels.

[45] G. I. Harris, A. K. Hyder, Jr., and J. Walinga, Bull. Am. Phys. Soc. **13**, 1372 (1968).
[46] J. B. French, Argonne National Laboratory Report No. ANL 6878 (unpublished).
[47] A. K. Hyder, Jr., G. I. Harris, J. J. Perrizo, and F. R. Kendziorski, Phys. Rev. **169**, 899 (1968).
[48] L. W. Nordheim, Phys. Rev. **78**, 294 (1950).
[49] K. Dong-Hyok, J. Phys. Soc. of Japan **21**, 2445 (1966).

and $(s_{1/2}p_{3/2})$ or $(d_{3/2}p_{3/2})$ admixtures in the 2^- and 3^- levels. [One expects the 5^- levels to be nearly pure $(d_{3/2}f_{7/2})$.] It is clear, for example, that the 2^- and 4^-, $T=1$ levels must have significant components of $(s_{1/2}p_{3/2})$ and $(s_{1/2}f_{7/2})$, respectively, since they are formed as strong resonances in proton capture by Si^{29}. Preliminary shell-model calculations[50] of odd-parity states in $A=29$ and 30 nuclei using a modified surface δ interaction do indeed show that the experimental spectrum is much more complicated than pure $(d_{3/2}f_{7/2})$. The $T=0$, 2^-, and 5^- levels can be explained as primarily of the type $(d_{3/2}f_{7/2})$, but the 3^- ($T=0$ and 1) and the 4^-, $T=0$ levels must be mainly $(s_{1/2}f_{7/2})$. Calculations of the $M1$ transition rates support this conclusion.

Additional evidence for the more complex character of the spectrum is provided by a comparison with the well-known ground-state $(d_{3/2}f_{7/2})$ n-p two-particle spectrum of Cl^{38}. As pointed out by French,[46] to within a J-independent constant, the energies of the levels of the n-p spectrum should be related to those of the two-nucleon spectrum as follows:

$$E_J^{(np)}=\tfrac{1}{2}[E_J(T=1)+E_J(T=0)].$$

The spectrum which results from the application of this relation to the P^{30} spectrum of Fig. 25 is compared with the known n-p spectrum of Cl^{38} in Fig. 26. The experimental Cl^{38} spectrum is arbitrarily adjusted to make its 2^- ground state coincide in energy with the 2^- level of the derived P^{30} spectrum. The two 5^- levels are seen to match very well; however, the 3^- and 4^- levels of the derived spectrum are 1.2–1.3 MeV lower than expected if they are $(d_{3/2}f_{7/2})$.

ACKNOWLEDGMENTS

We thank those of the Nuclear Structure Group who assisted with various portions of this work. We owe special thanks to D. V. Breitenbecher and W. A. Anderson for their invaluable assistance in the operation and maintenance of the accelerator and associated equipment. We are also indebted to P. Goldammer, S. Bergström-Rohlin, L. Meyer-Shutzmeister, J. P. Davidson, and P. W. M. Glaudemans for correspondence and discussions.

APPENDIX

In the main body of this paper, we have treated the 1505-keV resonance as a single level. As mentioned in the Introduction and in Sec. III, this resonance is in fact a very closely-spaced doublet with members having nearly identical properties. This discovery was made after the proton-capture work was completed, and during extensive high-resolution elastic proton-scattering measurements on $Si^{29}(p, p)Si^{29}$ with the ICT tandem accelerator which had just become available for experimental work. Since after detailed examination of the new results it became apparent that no significant changes in the discussions or conclusions of the main paper were necessary, it was decided to present here a separate discussion of the doublet (split analog) nature of this resonance.

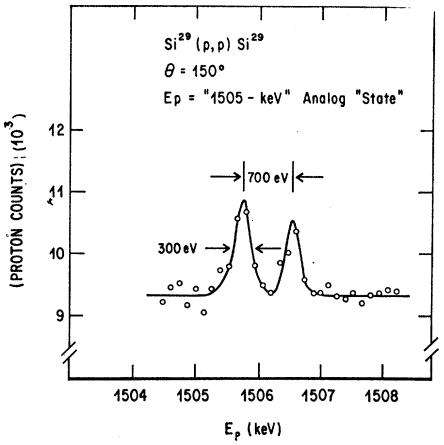

FIG. 27. Elastic proton-scattering results at $\theta(\text{lab})=150°$ in the neighborhood of the $T=1$ analog state near $E_p=1505$ keV in Si^{29}+p. Both resonances shown have $J^\pi=4^-$ and otherwise nearly identical properties. See Table XVI.

Details of the experimental setup and methods of analysis for the high-resolution elastic-scattering experiments will be published.[17] Figure 27 presents the sum of several runs with a very thin target (total energy spread$\simeq$300 eV) over the 1505-keV resonance region at an angle of $\theta_{\text{lab}}=150°$. These data show the existence, resolution, and separation of the doublet. Another run at three angles with a target of about 500 eV thickness and obtained with better statistics over a shorter time period was more suitable for analysis. The final result is that both resonances correspond to f-wave scattering with $J=2$ or 4. The $J=4$ assignment is more likely since, for $J=2$, p-wave would be expected to dominate over f-wave scattering.

If the resonances have different spins, then one would expect significant differences in the γ-ray decay schemes. On the other hand, if the two resonances arise from mixing of the analog state via the Coulomb interaction with a nearby $T=0$ level of the same spin and parity, the wave functions may be nearly identical, but orthogonal, combinations of the same basis states. In this case, the γ-ray decay schemes could be nearly identical. Because of the unusual and unique nature of the combined decay scheme (Fig. 7), there are therefore strong reasons to conclude that both resonances have the same J^π if they are found to have nearly identical decay schemes.

γ-ray spectra were obtained from each resonance with a 40-cc Ge(Li) detector using a target about 400 eV thick evaporated onto a thick (0.010-in.) silver backing. These measurements were performed by fixing the

[50] D. D. Watson and G. I. Harris, in Contributions to the International Conference on Properties of Nuclear States, Montreal, Canada, 1969 (unpublished).

TABLE XVI. Properties of the members of the doublet near $E_p=1505$ keV in $Si^{29}+p$. The results given are derived from combined proton-capture and elastic proton-scattering data.

E_p (keV)	J^π	Γ_γ (eV)	Γ_p (eV)	θ_p^2 ($l=3$)
1505.8±0.3	4^-	0.32±0.06	15±2	0.05
1506.5±0.3	4^-	0.24±0.05	22±2	0.08

accelerator beam energy at a value near the doublet and by setting the effective energy by means of a manually adjustable target-bias voltage obtained from a ±2-kV power supply. In this manner, it was possible to quickly check the bombarding energy relative to the resonance position, and to compensate for small drift during the runs. In addition, short runs alternated from one resonance to the other were used to compensate for long-term effects. The resulting γ-ray spectra were of poorer quality than the usual spectra obtained in this work because of the very thin target, low beam current ($\simeq$0.7 μA), and the need to limit the total running time. However, each spectrum clearly exhibited all but the very weakest transitions shown in Fig. 7. Furthermore, a detailed comparison showed no detectable differences in relative intensity of the various transitions in the two spectra. Variations in relative intensities of about 20% would have been observable for most transitions. Both resonances must therefore be 2^- or both 4^-. It is now apparent that both members of the doublet must have $J^\pi=4^-$, since the extensive angular-correlation data discussed in Sec. V C and in Ref. 4 on the combined resonances are entirely consistent with $J_R=4$, but are in clear disagreement with $J_R=2$.

The properties of both members of the doublet as determined from the combined (p, p) and (p, γ) data are listed in Table XVI. The resonance energies were determined by a special calibration of the NMR frequency for the 90° analyzing magnet of the tandem accelerator with the 991.90±0.04 keV resonance[51] in $Al^{27}(p, \gamma)Si^{28}$. The quoted energies have been corrected for relativistic effects. The energy of the lower member of the doublet ($E_p=1505.8\pm0.3$ keV) is in agreement with our previously adopted value of 1505±2 keV for the "resonance" energy. The doublet separation is 0.7±0.1 keV.

A final comment is necessary on the validity of the analysis of angular-correlation and polarization data in Secs. V and VI obtained on the unresolved doublet. For $J^\pi=4^-$, the resonance formation is by pure f-wave capture since h-wave capture can be safely ignored in the present circumstances. Thus, the population parameters of both resonances are fixed at $P(0)=0.44$ and $P(1)=0.56$. The multipolarity mixings, however, of corresponding primary transitions could be different. The near identity in all other respects of the two resonances causes one to believe they are not significantly different. We note that the measured mixing ratios of the six combined primary transitions (Table XII) vary in magnitude between $\delta=0.00$ and 0.08 with errors of ±0.02 or ±0.03. It seems highly unlikely that this set of consistently small values would be obtained if some of the independent mixing ratios were significantly large. This set of small observed mixing ratios can also be regarded as strong support for the conclusion that the resonances have the same J^π. All the evidence combined supports the general conclusion that the doublet corresponds to a $(J^\pi, T)=(4^-, 1)$ analog state which, via the Coulomb interaction, is almost completely mixed with a nearby $(J^\pi, T)=(4^-, 0)$ level. This result seems surprising in light of the relatively low observed density of states of the same J^π in the excitation region studied.

[51] J. B. Marion, Rev. Mod. Phys. **38**, 660 (1966).